Binary H_2SO_4-H_2O homogeneous nucleation based on kinetic quasi-unary nucleation model: Look-up tables

Fangqun Yu

Atmospheric Sciences Research Center, State University of New York at Albany, Albany, New York, USA

Received 11 June 2005; revised 7 September 2005; accepted 28 October 2005; published 17 February 2006.

[1] Recently, we have shown that the binary homogeneous nucleation (BHN) of H_2SO_4 and H_2O can be treated as a quasi-unary nucleation (QUN) of H_2SO_4 in the equilibrium with H_2O vapor and have developed a kinetic H_2SO_4-H_2O nucleation model, which simulates the dynamic evolutions of cluster distributions explicitly. In this paper we present improved and updated version of the QUN model, which has been modified through the incorporation of more rigorous thermodynamics of the cluster formation and the effect of the surface area of preexisting particles on nucleation rates. The difference in the model predictions of the improved and original QUN models is not dramatic; however, the improved QUN model is more consistent thermodynamically. The predicted BHN rates based on the QUN model are in good agreement with existing observations within the range of uncertainties. We also study the dependence of kinetic BHN rates on key input parameters and discuss the conditions in which the H_2SO_4-H_2O homogeneous nucleation in the atmosphere may become significant. The nucleation rates look-up tables derived from the QUN model, which can be readily used to find the nucleation rates at given conditions, are presented. The look-up tables cover a wide range of key parameters that can be found in the ambient atmosphere, in the laboratory studies, and in the exhaust plumes. These look-up tables can be easily incorporated in multidimensional models to predict BHN rates, and they can be utilized directly for the analysis and interpretation of the observed nucleation events.

Citation: Yu, F. (2006), Binary H_2SO_4-H_2O homogeneous nucleation based on kinetic quasi-unary nucleation model: Look-up tables, *J. Geophys. Res.*, *111*, D04201, doi:10.1029/2005JD006358.

1. Introduction

[2] Atmospheric particles affect regional air quality, human health, and climate, and these effects depend strongly on the number size distributions and compositions of the aerosols. The number size distributions of atmospheric aerosols are determined by a number of microphysical processes, of which the nucleation process is critical. Understanding the key microphysics controlling the formation and fate of secondary particles and representing these processes in the models are important to improving simulations of environmental and climatic impact of atmospheric aerosols.

[3] Gaseous H_2SO_4 and H_2O are active nucleation agents because the vapor pressure over the binary H_2SO_4-H_2O solution is very low. In addition to the binary H_2SO_4-H_2O homogeneous nucleation, which has been extensively studied for decades [e.g., *Doyle*, 1961; *Heist and Reiss*, 1974; *Jaecker-Voirol et al.*, 1987; *Kulmala et al.*, 1992; *Wilemski and Wyslouzil*, 1995; *Noppel et al.*, 2002], ternary nucleation (H_2SO_4-H_2O-NH_3) [e.g., *Coffman and Hegg*, 1995; *Korhonen et al.*, 1999; *Napari et al.*, 2002], ion-mediated nucleation (H_2SO_4-H_2O-ion) [*Yu and Turco*, 2000, 2001; *Yu*, 2002; *Eichkorn et al.*, 2002; *Laakso et al.*, 2002; *Lee et al.*, 2003; *Kazil and Lovejoy*, 2004; *Wilhelm et al.*, 2004], and organic enhanced nucleation (H_2SO_4-H_2O-organic) [*Zhang et al.*, 2004] have been proposed as possible alternative mechanisms of the nucleation in the atmosphere. Nevertheless, binary homogeneous nucleation (BHN) of H_2SO_4-H_2O is the basis of all these recent nucleation theories and it may dominate the nucleation in certain atmospheric regions or under favorable conditions. Despite decades of the intensive research on the classical theory of homogeneous nucleation, the agreement between theoretical predictions and experimental data for both the unary [e.g., *Nadykto and Yu*, 2005] and binary nucleation [e.g., *Vehkamäki et al.*, 2002] is still not always satisfactory.

[4] The classical BHN theory expresses the nucleation rate as [*Reiss*, 1950], $J = C \exp(-\Delta G^*/kT)$, where C is a frequency factor and ΔG^* is the free energy required to form a critical cluster. Sulfuric acid molecules tend to form hydrates, which are believed to stabilize the cluster and hinder the nucleation. The hydration effect, which has been taken into account in the improved version of the BHN theory [e.g., *Heist and Reiss*, 1974; *Jaecker-Voirol et al.*, 1987; *Noppel et al.*, 2002], reduces the nucleation rates by a

0148-0227/06/2005JD006358$09.00

factor of $\sim 10^3 - 10^8$. The equilibrium cluster size distribution on which the classical BHN theory is based is known to violate the mass action law and it mismatches the equilibrium cluster distribution for monomers [*Wilemski*, 1975; *Wilemski and Wyslouzil*, 1995]. Several attempts to correct these inconsistencies [*Kulmala et al.*, 1992; *Wilemski and Wyslouzil*, 1995] have been made in the past; however, the validity of these corrections has not been fundamentally justified, and thus the unified binary cluster distribution remains to be established.

[5] Different versions of the classical BHN theory have been widely used to calculate the production rates of new particles in the atmosphere [e.g., *Mirabel and Katz*, 1974; *Hamill et al.*, 1982; *Kreidenweis and Seinfeld*, 1988; *Russell et al.*, 1994; *Andronache et al.*, 1997; *Clarke et al.*, 1999; *Adams and Seinfeld*, 2002; *ENVIRON*, 2004]. The key step in calculating the BHN rates of H_2SO_4-H_2O is to locate the saddle point on the two-dimension surface of Gibbs free energy change or, in the other words, to determine the size and composition of the critical clusters. In order to reduce the computational time and facilitate the analysis of the observed nucleation events, the nucleation rates of H_2SO_4-H_2O has been parameterized [*Wexler et al.*, 1994; *Russell et al.*, 1994; *Capaldo et al.*, 1999; *Kulmala et al.*, 1998; *Vehkamäki et al.*, 2002].

[6] The work by *Vehkamäki et al.* [2002] is based on the refinements of the nucleation rate calculations, following the work by *Kulmala et al.* [1998] and *Noppel et al.* [2002]. *Vehkamäki et al.*'s [2002] parameterization gives nucleation rates $10-10^4$ higher than *Kulmala et al.*'s [1998] parameterization. *Vehkamäki et al.*'s [2002] parameterization, which is based on the most rigorous nucleation kinetics and thermodynamically consistent version of the classical BHN theory, could be considered as the best of its kind currently available. Nevertheless, *Vehkamäki et al.* [2002] showed that the nucleation rates predicted with their parameterization are generally several orders of magnitudes higher than the laboratory measurements reported by *Viisanen et al.* [1997] and *Ball et al.* [1999].

[7] Recently, *Yu* [2005] showed that the binary homogeneous nucleation (BHN) of H_2SO_4 and H_2O can be treated as quasi-unary nucleation (QUN) of H_2SO_4 in the equilibrium with water vapor and developed a kinetic H_2SO_4-H_2O homogeneous nucleation model. In the kinetic QUN model, the growth and evaporation of sulfuric acid-water clusters of various sizes are simulated explicitly. The kinetic QUN model, in which cluster distributions are simulated kinetically, is fundamentally different from the classical BHN model based on the assumed statistical equilibrium cluster distribution. The QUN model does not have two well-known problems associated with the classical BHN theory (violation of mass action law and incorrect monomer concentration given by cluster distributions) and is appropriate for the situations, such as in rapidly diluting engine exhaust (H. Du and F. Yu, Formation of volatile nanoparticles in engine exhaust: Contributions of the binary H_2SO_4-H_2O homogeneous nucleation, submitted to Atmospheric Environment, 2006, hereinafter referred to as Du and Yu, submitted manuscript, 2006), when the assumption about the steady state equilibrium cluster distribution is no longer valid.

[8] In this paper we present the improved and extended version of the QUN model, which is based on the more rigorous treatment of the thermodynamics of the cluster formation and takes the effect of preexisting particles on nucleation rates into account. We perform a comprehensive sensitivity study of H_2SO_4-H_2O homogeneous nucleation rates to key input parameters and discussed the conditions, in which the binary nucleation of the sulfuric acid and water may become significant. We also present the look-up tables derived using the improved QUN model, which cover a wide range of the key input parameters for a variety of conditions including those in the ambient atmosphere, laboratory conditions, and exhaust plumes.

2. A Kinetic Model of H_2SO_4-H_2O Quasi-Unary Nucleation

[9] The key assumptions of the kinetic H_2SO_4-H_2O QUN model [*Yu*, 2005] include the following: (1) At given temperature (T) and relative humidity (RH), the sulfuric acid clusters of various sizes are in equilibrium with water and their average compositions (i.e., number of H_2O molecules i_b in a cluster containing i_a H_2SO_4 molecules) can be approximated using the most stable compositions. (2) The binary H_2SO_4-H_2O nucleation is controlled by the growth/shrink of $(H_2SO_4)_{i_a}$ $(H_2O)_{i_b}$ clusters (named i_a−mers thereafter) through the uptake/evaporation of H_2SO_4 molecules. The QUN model effectively decouples the two-dimension nucleation problem into a one-dimensional problem that allows obtaining the explicit time-dependent picture of the evolution of pre-nucleation clusters in the nucleating vapors.

[10] The equilibrium (or average) number of H_2O molecules in the i_a-mer (i.e., $i_b(i_a)$) is a function of T and RH only. $i_b(i_a)$ is determined by locating the minimum point of the change in the Gibbs free energy $\Delta G(i_a, i_b)$ in i_b direction [*Yu*, 2005]. This approach is equivalent to solving the following Kelvin equation ($\zeta = b$ for water) for the equilibrium cluster composition [*Doyle*, 1961]

$$\Delta\mu_\zeta + \frac{2\sigma v_\zeta}{r} + \frac{3(1-X_\zeta)v}{r}\frac{d\sigma}{dX_\zeta} = 0, \tag{1}$$

where

$$\Delta\mu_\zeta = -k_B T \ln\left(\rho_\zeta^{free}/\rho_{\zeta,s}^{free}\right) \tag{2}$$

is the difference in the chemical potential for molecules of species ζ ($\zeta = a$ for sulfuric acid and $= b$ for water) in the solution and in the vapor phase. Here ρ_ζ^{free} and $\rho_{\zeta,s}^{free}$ are the number concentrations of free molecules of component ζ in the vapor phase and in the saturated vapor above a flat surface of a solution having the same composition as the cluster, respectively. X_ζ is the molar fraction specie ζ in the cluster. Here σ is the surface tension of the binary solution, r is the cluster radius, v_ζ is the partial molecular volume of specie ζ, v is the average molecular volume, and k_B is the Boltzmann's constant. The bulk cluster density and surface tension are calculated using parameterizations of *Vehkamäki et al.* [2002]. In our model $\rho_{\zeta,s}^{free}$ is calculated using the

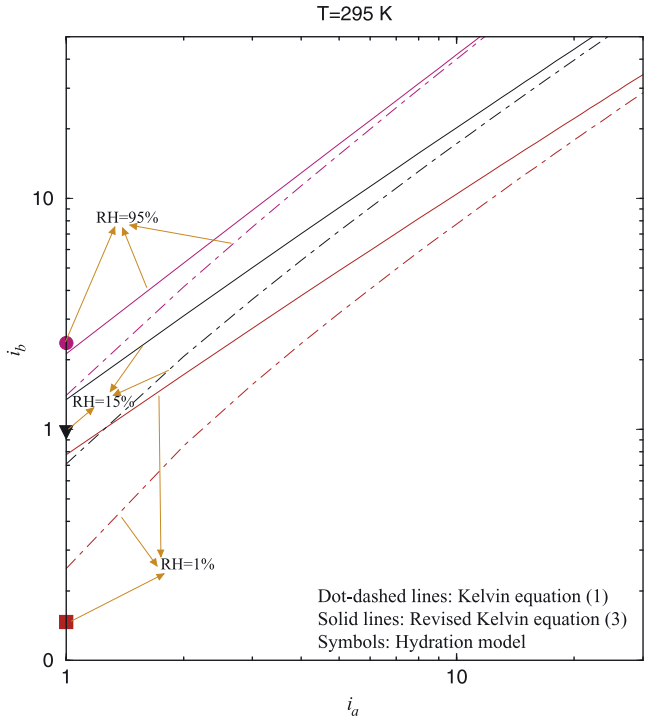

Figure 1. Equilibrium (or average) numbers of water molecules (i_b) in i_a−mers at RH = 1%, 15%, and 95% calculated based on the Kelvin equation with (equation (1), dot-dashed lines) and without (equation (3), solid lines) surface tension derivative term. The symbols are $i_b(1)$ calculated from the hydration model (equation (5)). The temperature is 295 K.

parameterization of *Taleb et al.* [1996] with the pure acid saturation vapor pressure given by [*Ayers et al.*, 1980; *Kulmala and Laaksonen*, 1990; *Noppel et al.*, 2002],

$$p_{acid}^{pure}(\text{in Pa}) = 101325 \times e^{\left\{L+10156\left[\frac{1}{360.15}-\frac{1}{T}+\frac{0.38}{545}(1+\ln(360.15/T)-360.15/T)\right]\right\}} \quad (2a)$$

[11] The value of L given by *Kulmala and Laaksonen* [1990] is −11.94. In the work of *Noppel et al.* [2002], two additional values of L (−11.695 and −11.387) were derived. In the calculations presented in this paper, we used $L = -11.695$ which is close to the average of the three L values. The calculated nucleation rates are about 1–2 orders of magnitude higher if $L = -11.94$ and 1–2 orders of magnitude lower if $L = -11.387$. Owing to the uncertainties in the experimental results and the hydration calculation (see discussion below in this section), it is difficult to tell at this point which L value gives more accurate results.

[12] The derivation of equation (1) has been performed using the Gibbs-Duhem identity [*Doyle*, 1961] and clusters were assumed to be of a uniform bulk composition. However, it has been found that the composition of cluster surface layer may differ significantly from the bulk due to surface enrichment or adsorption [*Wilemski*, 1987; *Mirabel and Reiss*, 1987; *Laaksonen et al.*, 1999]. In the case, when the surface and bulk (or interior) molecules in the cluster are distinguished, the surface derivative term in equation (1) is eliminated by using the Gibbs adsorption isotherm that leads to the following revised Kevin equations for the binary mixture [*Renninger et al.*, 1981]

$$\Delta\mu_\zeta + \frac{2\sigma v_\zeta}{r} = 0. \quad (3)$$

[13] Revisited Kelvin equations (3) are consistent thermodynamically and thermodynamic properties of the solution should be evaluated based on the cluster composition defined by equations (3) [*Renninger et al.*, 1981; *Wilemski*, 1987; *Mirabel and Reiss*, 1987; *Laaksonen et al.*, 1999; *Noppel et al.*, 2002].

[14] For clusters containing one sulfuric acid molecule (i.e., acid monomers), the average composition can also be calculated using the hydration model. The concentration of sulfuric acid molecules associated with h water molecules (n_1^h) is given by the following equation [*Jaecker-Voirol et al.*, 1987; *Noppel et al.*, 2002]

$$n_1^h = \rho_a^{free} K_1 K_2 \ldots K_h \left(\frac{\rho_w^{free}}{\rho_0}\right)^h, \quad (4)$$

where K_h are the equilibrium constants for the successive additions of water molecules to an acid molecule, which are calculated at the reference vapor concentration ρ_0.

[15] According to the hydration theory, the average number of water molecules associated with a sulfuric acid monomer is

$$i_b(1) = \frac{K_1\left(\frac{\rho_w^{free}}{\rho_0}\right) + 2K_1K_2\left(\frac{\rho_w^{free}}{\rho_0}\right)^2 + \ldots + hK_1K_2\ldots K_h\left(\frac{\rho_w^{free}}{\rho_0}\right)^h}{F_{hy}}, \quad (5)$$

where

$$F_{hy} = \frac{\rho_a^{total}}{\rho_a^{free}} = 1 + K_1\left(\frac{\rho_w^{free}}{\rho_0}\right) + K_1K_2\left(\frac{\rho_w^{free}}{\rho_0}\right)^2 + \ldots + K_1K_2\ldots K_h\left(\frac{\rho_w^{free}}{\rho_0}\right)^h \quad (6)$$

is the ratio of the total concentration of sulfuric acid hydrates $\left(\rho_a^{total} = n_a = n_1 = \sum_{j=0}^{h} n_1^j\right)$ to the number concentration of free (nonhydrated) sulfuric acid ($\rho_a^{free} = n_1^0$).

[16] Figure 1 shows the equilibrium (or average) numbers of water molecules (i_b) in i_a-mers at RH = 1%, 15%, and 95% calculated based on the Kelvin equation with (equation (1), dot-dashed lines) and without (equation (3), solid lines) term related to the derivative of the surface tension. The symbols in Figure 1 are $i_b(1)$ values calculated from the hydration model (equation (5)). The equilibrium constants (K_1–K_5) used here were derived by *Noppel et al.* [2002] using activity coefficients from *Clegg and Brimblecombe* [1995]. The ambient temperature is 295K. As seen from Figure 1, equation (3) predicts higher water content for all the clusters than equation (1). The relative difference is large at small i_a and low RH. In the revised QUN model, equation (3) is used to calculate the cluster compositions.

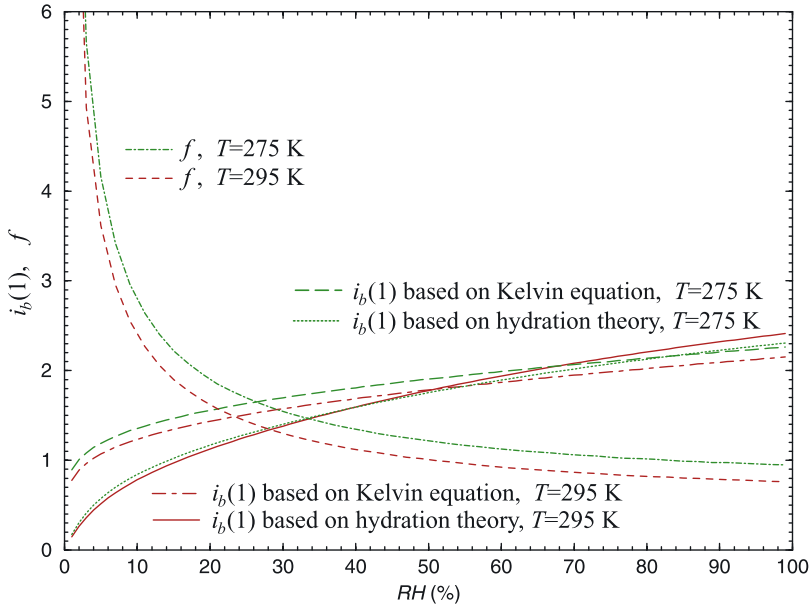

Figure 2. Average number of water molecules associated with sulfuric acid monomer (i.e., $i_b(1)$) calculated with Kelvin equation (equation (3)) and hydration theory (equation (5)), and the equilibrium constant modification factor f ($K_h' = f\,K_h$) required to make the hydration theory give the same $i_b(1)$ as Kelvin equation.

[17] There is also considerable difference between average compositions of acid monomers using the Kelvin equation and those based on hydration theory, especially at lower *RH*s. Since both approaches feature significant uncertainties, it is difficult to figure out which method gives more realistic values. The accuracy of the Kelvin equation applied for the estimations of the average compositions of acid monomers depends strongly on the validity of the capillary approximation in the case of nano-sized systems such as molecular clusters. On the other hand, the predictivity of the hydration theory is limited by large uncertainties in the values of K_h, which are not well defined. *Noppel et al.* [2002] presented a comprehensive list of K_h values computed using different methods such as liquid droplet model, ab initio calculations, and parameterization of the experimental data, and he showed that divergence in the K_h values is excessively large. For example, different versions of liquid drop model differ in K_1 by a factor of ~6.8.

[18] Since in our model the compositions of all clusters containing more than one H_2SO_4 molecules are derived from the Kelvin equation, it appears to be more consistent to use the acid monomer composition calculated from the Kelvin equation as well (otherwise, there is a jump in the composition change from acid monomers to acid dimmers). We found that the hydration theory gives the same acid monomer compositions as those calculated based on the Kelvin equation when the values of K_h are scaled with the factor f,

$$K_h^{'} = fK_h. \tag{7}$$

[19] The values of f are obtained by matching $i_b(1)$ calculated from hydration theory with equilibrium constants K_h' to those based on Kelvin equation (equation (3)). Figure 2 shows f as a function of *RH* at T = 295 K and 275 K, along with $i_b(1)$ calculated based on Kelvin equation (equation (3)) and hydration theory (equation. (5), no modification in K_h). As may be seen from Figure 2, f decreases with *RH* and is in the range of 0.75–2.0 at RHs > ~15% that is within the divergence range of K_h values. Figure 2 also shows that the Kelvin equation predicts much stronger hydration of sulfuric acid monomers at lower *RH*s and weaker dependence of the hydration number on *RH*s than the hydration theory. Uncertainties in K_h are known to lead to uncertainty of many orders of magnitude in the nucleation rates [*Noppel et al.*, 2002]. We will show below that accounting for the hydration effect calculated using K'_h defined by equation (7) leads to a better agreement with experimental results. In the revised QUN model, K'_h is used to calculate monomer hydration.

[20] When the compositions of clusters $i_b(i_a)$ are known, other cluster properties (radius r_{i_a}, mass m_{i_a}, bulk density and surface tension, etc.) can be decided accordingly. The time-dependent evolution of cluster size distributions can be obtained by solving the following set of the differential equations:

$$\frac{dn_{i_a}}{dt} = \delta_{i_a-1,1}\beta_{i_a-1}n_{i_a-1} - \gamma_{i_a}n_{i_a} - \beta_{i_a}n_{i_a} + \gamma_{i_a+1}n_{i_a+1} - n_{i_a}\sqrt{\frac{k_BT}{2\pi m_{i_a}}}S, \quad i_a \geq 2 \tag{8}$$

$$\frac{dn_1}{dt} = P - \sum_{i_a=1}^{\infty}\beta_{i_a}n_{i_a} + 2\gamma_2 n_2 + \sum_{i_a=3}^{\infty}\gamma_{i_a}n_{i_a} - n_1\sqrt{\frac{k_BT}{2\pi m_1}}S, \tag{9}$$

where n_{ia} is the number concentration of clusters containing i_a H_2SO_4 molecules (and $i_b(i_a)$ H_2O molecules). P is the

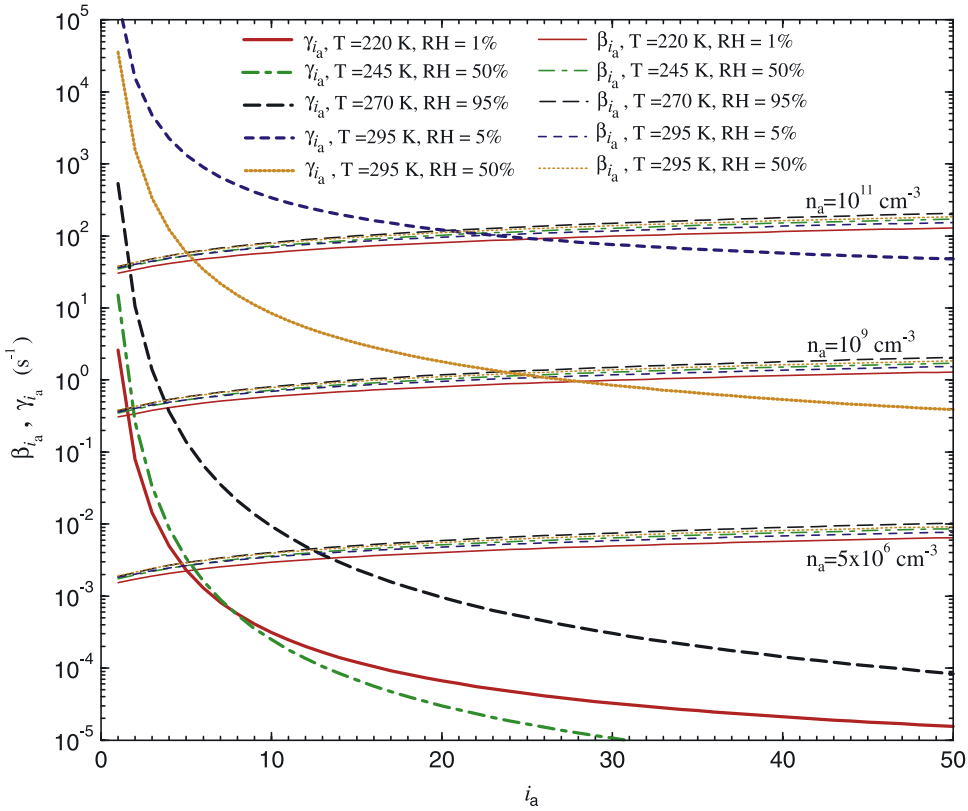

Figure 3. The forward (or growth) rate coefficient (β_{i_a}) and the reverse (or evaporation) rate coefficient (γ_{i_a}) of i_a-mers as a function of i_a at five different atmospheric conditions. Here β_{i_a} is given at three H_2SO_4 vapor concentrations ($n_a = 5 \times 10^6$, 10^9, 10^{11} cm^{-3}). The intersection points of β_{i_a} and γ_{i_a} curves are the locations of critical clusters.

production rate of H_2SO_4 molecules. S is the characteristic surface area of the preexisting particles. Here β_{i_a} is the forward (or growth) rate of i_a-mers, and γ_{i_a} is the reverse (or evaporation) rate of H_2SO_4 molecules from i_a-mers. $\delta_{i_a-1,\,1} = 1$, when $i_a > 2$ and $= 0.5$ when $i_a = 2$. The coagulation among clusters is not considered in equation (8), which is a good approximation in the case when $n_1 \gg n_{i_a}$ ($i_a > 1$).

[21] The effect of the preexisting particles on the nucleation by scavenging precritical clusters (equation (8)), which is not considered in the earlier version of QUN model [*Yu*, 2005] and not treated in the classical BHN as well, is included in the revised QUN model presented in this paper. In the past, the modeling studies of the effect of preexisting particles on BHN were limited to the scavenging of precursor gases by these particles only (equation (9)).

[22] The detailed description of methods used to calculate β_{i_a} and γ_{i_a} have been presented by *Yu* [2005]. The forward rate β_{i_a} is the kinetic collision rate of monomers (free + hydrated) of the number concentration $n_1 = \rho_a^{total}$ with i_a-mers

$$\beta_{i_a} = \left(\frac{8\pi k_B T(m_1 + m_{i_a})}{m_1 m_{i_a}}\right)^{1/2} (r_1 + r_{i_a})^2 n_1. \qquad (10)$$

[23] Evaporation rate γ_{i_a} is calculated based on the assumption that the cluster reverse (evaporation) rate is equal to the forward (growth) rate, when clusters are in equilibrium with surrounding H_2SO_4 vapor. In the revised QUN model, γ_{i_a} is expressed as

$$\gamma_{i_a} = \beta_{i_a} \frac{\rho_{a,s}^{total}}{\rho_a^{total}} \exp\left(\frac{2\sigma v_a}{k_B T r_{i_a}}\right), \qquad (11)$$

where $\rho_{a,s}^{total}$ is the total number concentrations of H_2SO_4 molecules in the saturated vapor above a flat surface of the binary solution of the same composition as the cluster composition. R is the general gas constant. On the basis of the hydration theory, $\rho_{a,s}^{total}$ is related to $\rho_{a,s}^{free}$ as,

$$\rho_{a,s}^{total} = F_{hy} \rho_{a,s}^{free}, \qquad (12)$$

where F_{hy} is defined in equation (6) and $\rho_{a,s}^{free}$ is calculated using the parameterization given by *Taleb et al.* [1996].

[24] The formula to calculate γ_{i_a} in the revised QUN model (equation (11)) differs from the earlier one [*Yu*, 2005] in that (1) the hydration effect is now considered in the calculations of γ_{i_a}, (2) the H_2SO_4 partial molecular volume is used instead of H_2SO_4 average molecular volume.

[25] Figure 3 shows γ_{i_a} and β_{i_a} as a function of i_a at five different atmospheric conditions. The values of β_{i_a} corresponding to three different H_2SO_4 vapor concentrations ($n_1 = n_a = 5 \times 10^6$, 10^9, and 10^{11} cm^{-3}) are presented.

The average composition of sulfuric acid monomers is based on Kelvin equation (3) and F_{hy} is calculated using K'_h defined by equation (7). Here β_{i_a} is proportional to n_a, while γ_{i_a} is independent of n_a. γ_{i_a} is very sensitive to T and RH, while the effect of the T and RH on β_{i_a} is small. The intersection points of β_{i_a} and γ_{i_a} curves show the location of the critical clusters. Therefore the properties of critical clusters (number of sulfuric acid molecules i_a^*, radius r^*, acid mole fraction x^*, etc.) can be decided in a straightforward way in the kinetic QUN model.

[26] The evolution of cluster size distributions (n_{i_a}) can be obtained by solving the kinetic cluster dynamic equations (8)–(9), even if T, RH and n_a change rapidly (such as in diluting exhaust plume). In many applications, a steady state nucleation rate at given n_a is needed. In the simulations presented below, we assume a constant n_a (or n_1) and solve equation (8) to obtain the steady state cluster distribution and nucleation rate. An upper limit cluster size of i_a = 100 is used. The largest cluster is allowed to grow over the boundary i_a = 100, but no clusters return by evaporation from i_a > 100. The critical clusters generally contain less than 20 H_2SO_4 molecules when the nucleation rates are not negligible and the simulated results do not change when larger upper limit cluster size is used. A semi-implicit scheme (similar to that discussed by *Jacobson et al.* [1994] for solving aerosol coagulation equations) is used to solve cluster kinetic equations. The semi-implicit scheme conserves the total sulfuric acid mass in the system, for example, $\sum_{i_a=1}^{\infty} i_a^* n_{i_a}$ = constant = n_a when n_1 is not set as constant and P = 0, S = 0. The time step used in the numerical calculation depends on β_1 (or n_1) ($\Delta t = 0.0003/\beta_1$), and the change in the predicted nucleation rates is very small when a smaller time step is used. Figure 4 shows the evolution of cluster size distributions for three cases: T = 220 K, RH = 1%, $n_a = 5 \times 10^6$ cm^{-3}, and S = 100 μm^2/cm^3 (Figure 4a); T = 270 K, RH = 95%, $n_a = 5 \times 10^7$ cm^{-3}, and S = 300 μm^2/cm^3 (Figure 4b); and T = 295 K, RH = 5%, $n_a = 3 \times 10^{11}$ cm^{-3}, and $S = 2 \times 10^5$ μm^2/cm^3 (Figure 4c). For comparison, the steady state cluster distribution at the same T, RH, and n_a but with S = 0 μm^2/cm^3 (solid line) is given in each panel. The arrow in each panel marks the location of the critical size (i_a^*). At t = 0 s, only monomers exist. The growth of clusters can be clearly seen from Figure 4. The concentrations of precritical clusters do not change further after t_s = ~1000 s, 100 s, and 0.1 s for Figures 4a, 4b, and 4c, respectively. In other words, the precritical clusters reach steady-state distribution (i.e., $\frac{dn_{i_a<i_a^*}}{dt} = 0$) after t_s. The time needed to reach steady state distribution of subcritical clusters (t_s) is inversely proportional to n_a.

[27] It is well known that preexisting particles in the atmosphere significantly influence the H_2SO_4 -H_2O nucleation rates through their effect on H_2SO_4 vapor concentration. However, it may be seen from Figure 4 that in the case, when the H_2SO_4 vapor concentration is constant, the effect of the preexisting particles on the size distributions of precritical clusters in typical atmospheric conditions is limited. The effect of the preexisting particles is larger, when monomer concentration is lower.

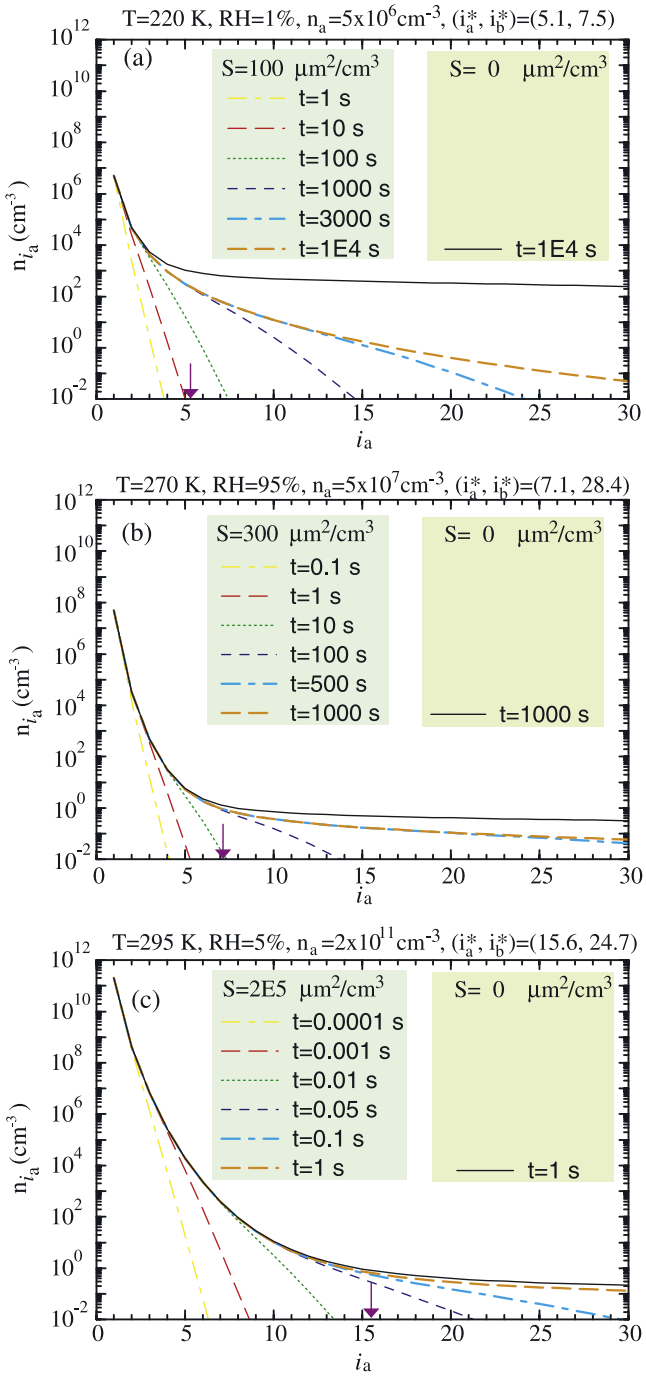

Figure 4. The evolution of cluster size distributions for three cases: (a) T = 220 K, RH = 1%, $n_a = 5 \times 10^6$ cm^{-3}, and S = 100 μm^2/cm^3; (b) T = 270 K, RH = 95%, $n_a = 5 \times 10^7$ cm^{-3}, and S = 300 μm^2/cm^3; and (c) T = 295 K, RH = 5%, $n_a = 3 \times 10^{11}$ cm^{-3}, and $S = 2 \times 10^5$ μm^2/cm^3. For comparison, the steady state cluster distribution under same T, RH, and n_a but with S = 0 μm^2/cm^3 (solid line) is also given in each panel. The arrow in each panel marks the location of the critical size (i_a^*). The concentration of H_2SO_4 monomer n_a (or n_1) is fixed during the simulations.

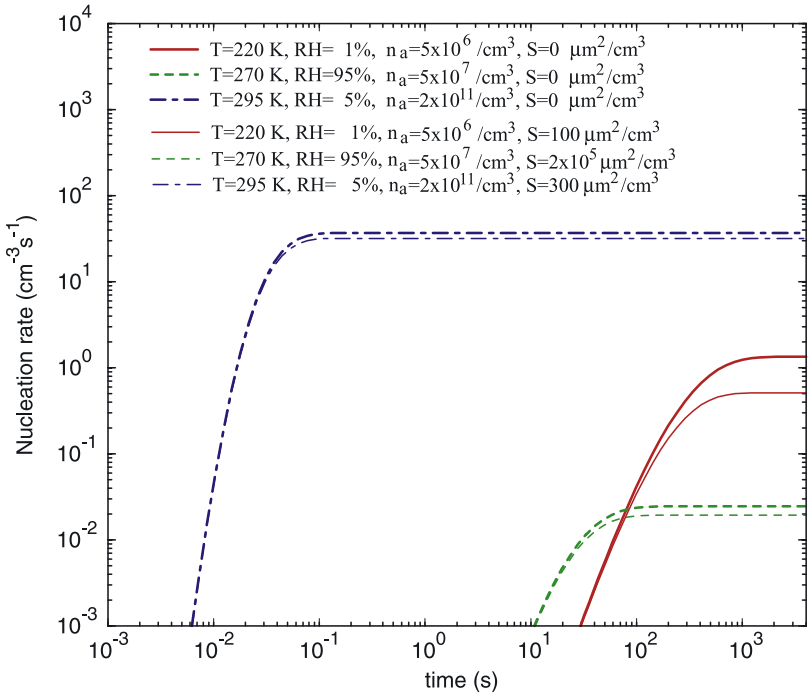

Figure 5. The kinetic quasi-unary nucleation rates of H_2SO_4-H_2O as a function of time for the cases shown in Figure 4.

[28] The nucleation rates in the kinetic QUN model (denoted as J_{QUN} and J'_{QUN}, when K_h and K'_h, respectively, are used in the calculations of the monomer hydration) are given by

$$J_{QUN} \text{ or } J'_{QUN} = \beta_{i_a^*} n_{i_a^*} - \gamma_{i_a^*+1} n_{i_a^*+1}. \quad (13)$$

[29] Figure 5 shows J'_{QUN} as a function of time corresponding to the cases shown in Figure 4. J'_{QUN} increases with time but it reaches steady-state values after some time (t_s). The steady state values of J'_{QUN} depend on T, RH, n_a, and S. It can be seen again that t_s is inversely proportional to H_2SO_4 monomer concentrations and the effect of preexisting particle surface area on nucleation rate for a given n_a is limited. For the nucleation rates shown in the following sections, the steady state values of the nucleation rates computed with the kinetic QUN model are used.

3. Dependence of H_2SO_4-H_2O BHN Rates on Key Parameters

[30] Figure 6 shows the nucleation rate as a function of sulfuric acid vapor concentration (n_a) at six different relative humidity and two different temperatures. The solid lines and long dashed lines are the nucleation rates predicted by the revised kinetic quasi-unary H_2SO_4-H_2O nucleation model with the monomer hydration calculated based on K_h (J_{QUN}) and K'_h (J'_{QUN}), respectively. The nucleation rates predicted by the most recent version of classical BHN theory (J_{CBHN}) [*Vehkamäki et al.*, 2002] are also shown for the comparison. The experimental data in Figures 6a–6b are from *Viisanen et al.* [1997] and those in Figures 6c–6f are from *Ball et al.* [1999].

[31] As seen from Figure 6, both J_{QUN} and J'_{QUN} are consistent with the experimental data within the range of uncertainties, while the classical BHN theory generally overpredicts the nucleation rates. J'_{QUN} is lower than J_{QUN} at low RHs and higher at higher RHs. The difference between J'_{QUN} and J_{QUN} is mainly caused by the difference in the degree of monomer hydration (see Figure 2), which affects the cluster evaporation rate (equation (11)). J_{CBHN} are consistently ~2–4 orders of magnitude higher than J_{QUN} under the conditions shown in Figure 6. This deviation is likely caused by the fundamental difference in the treatment of nucleation process (i.e., quasi-unary versus binary, kinetic versus classical, hydration of clusters of all sizes versus hydration of monomers only) as well as the difference in the water and acid activities used in the H_2SO_4-H_2O solution (we employed parameterization of *Taleb et al.* [1996], while *Vehkamäki et al.* [2002] used the parameterization by *Zeleznik* [1991]).

[32] The values of total concentration of H_2SO_4 molecules (n_a) required to produce a unit nucleation rate (1 cm^{-3} s^{-1}) as a function of RH, calculated with the revised kinetic QUN model (solid line: K'_h used; dashed line: K_h used) and the classical BHN model [*Vehkamäki et al.*, 2002] (dot-dashed line) at T = 298 K are presented in Figure 7. The symbols are experimental data from *Boulaud et al.* [1977] (T = 298 K), *Wyslouzil et al.* [1991] (T = 293 K), *Viisanen et al.* [1997] (T = 298 K), and *Ball et al.* [1999] (T = 295 K) with vertical bars showing the ranges of uncertainties. The curve based on classical BHN theory is generally beyond the lower edges of the uncertainty bars. On the other hand, both curves based on the kinetic QUN model are within the range of the uncertainties and curve calculated using the modified hydration equilibrium constants (K'_h) appears to be in a better agreement with the experimental results. All the results presented below are based on the kinetic QUN

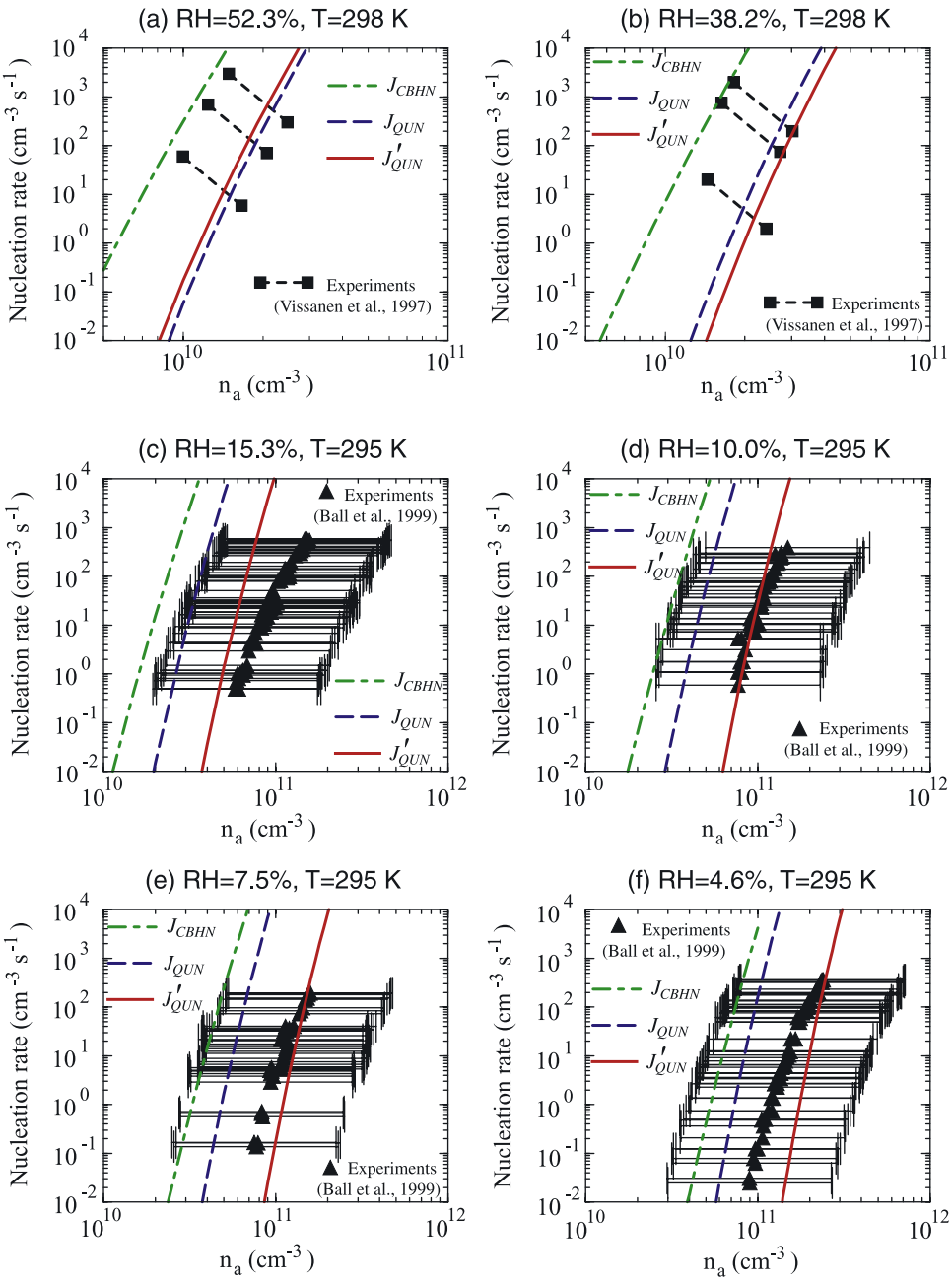

Figure 6. Nucleation rates as a function of sulfuric acid vapor concentration (n_a) at (a) $RH = 52.3\%$, $T = 298$ K, (b) $RH = 38.2\%$, $T = 298$ K, (c) $RH = 15.3\%$, $T = 295$ K, (d) $RH = 10.0\%$, $T = 295$ K, (e) 7.5%, $T = 295$ K, and (f) 4.6%, $T = 295$ K. The solid lines and long dashed lines are the nucleation rates predicted by the revised kinetic quasi-unary H_2SO_4-H_2O nucleation model with the monomer hydrates calculated based on K_h (J_{QUN}) and K'_h (J'_{QUN}), respectively. The predicted nucleation rates by the most recent version of classical BHN theory (J_{CBHN}) [*Vehkamäki et al.*, 2002] are also shown for comparison. The experimental data in Figures 6a–6b are from *Viisanen et al.* [1997] and in Figures 6c–6f are from *Ball et al.* [1999].

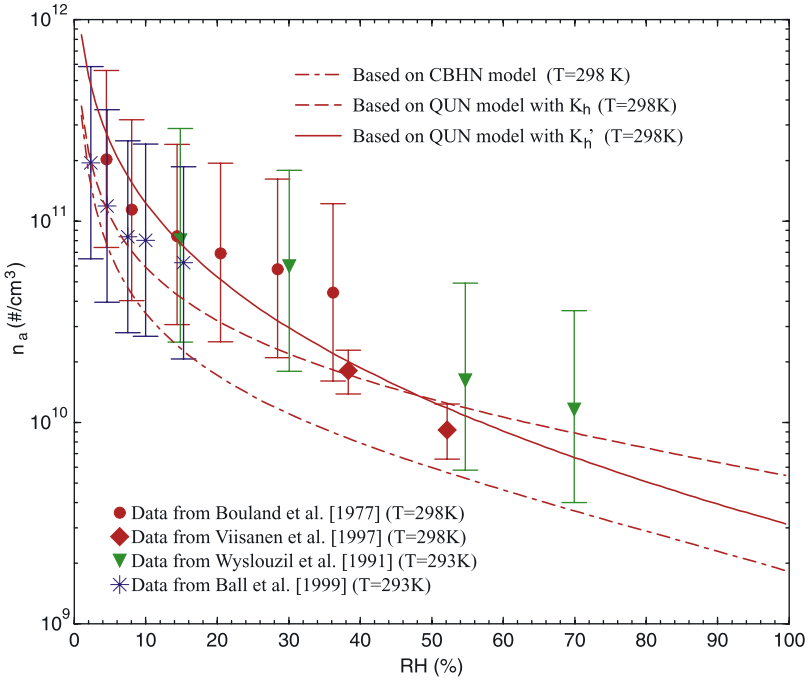

Figure 7. The values of total H_2SO_4 molecule concentration (n_a) required to give a unit nucleation rate (1 cm^{-3} s^{-1}) as a function of *RH*, calculated with the revised kinetic QUN model (solid line: K'_h used; dashed line: K_h used) and the classical BHN model [*Vehkamäki et al.*, 2002] (dot-dashed line) at T = 298 K. The symbols are experimental data from *Boulaud et al.* [1977] (T = 298 K), *Wyslouzil et al.* [1991] (T = 293 K), *Viisanen et al.* [1997] (T = 298 K), and *Ball et al.* [1999] (T = 295 K) with vertical bars showing the ranges of uncertainties.

model with monomer hydration calculation using K'_h, which give average monomer concentration in agreement with the Kelvin equation (3).

[33] Figure 8 shows the dependence of steady state nucleation rate (Figure 8a), number of H_2SO_4 molecules in the critical clusters (i^*_a) (Figure 8b), critical radius (r^*) (Figure 8c), and critical cluster acid mole fraction (x^*) (Figure 8d) on H_2SO_4 vapor concentration (n_a) predicted by the kinetic QUN model. Four curves in each panel represent four atmospheric conditions: the solid lines correspond to the stratospheric condition (T = 220K, *RH* = 1%), the short-dash and long-dashed lines refer to the middle-upper troposphere conditions (T = 240 K and 250 K, *RH* = 50%), and the dot-dashed lines refer to the conditions in the low cloud boundaries (T = 270 K, *RH* = 95%). The surface area of preexisting particles is set to 0. In order to reach the nucleation rate of >0.1/cm^3 s, which can be considered as significant, n_a has to be above 3×10^6, $2–10 \times 10^6$, and 5×10^7/cm^3 in the given stratospheric, middle-upper tropospheric, and low cloud boundaries conditions, respectively. Here n_a is typically <10^6/cm^3 in the background stratosphere but its value could reach above 3×10^6/cm^3 in volcano plumes. Thus H_2SO_4-H_2O homogeneous nucleation in the stratosphere is likely negligible but it could become significant in the volcano perturbed conditions. It is possible that n_a reaches above 2×10^6/cm^3 in the middle-upper troposphere and above 5×10^7/cm^3 in low cloud boundaries. Therefore H_2SO_4-H_2O BHN can contribute to new particle formation in these regions. Since T and *RH* in these regions may vary significantly from the model conditions discussed above, the corresponding nucleation rates at a given n_a may vary significantly. Figures 8b and 8c indicate that in order to reach significant nucleation rates the numbers of sulfuric acid in the critical clusters should be below 10 and radius of the critical cluster should not exceed 0.7 nm. The mole fraction of acid in the critical clusters depends strongly on *RH* (Figure 8d).

[34] The dependencies of J'_{QUN} on *RH* (at given T and n_a) and T (at given *RH* and n_a) are shown in Figures 9 and 10, respectively. Both T and *RH* affect the nucleation rates but the sensitivity of the nucleation rates to T or *RH* varies. J'_{QUN} is more sensitive to T or *RH* when J'_{QUN} is small that is generally associates with large i^*_a. J'_{QUN} becomes less sensitive to T or *RH,* when the size of critical clusters decreases. In the case when the nucleation is barrierless ($i^*_a \leq 2$), the nucleation rates are limited by monomer collision rates only and thus they are insensitive to changes in T and *RH*.

[35] The dependence of steady-state nucleation rates at given T, *RH*, and n_a on the surface area of the preexisting particles is presented in Figure 11. In the case, when the acid vapor number concentration is constant, the effect of preexisting particles on nucleation through scavenging precritical clusters ($2 \leq i_a \leq i^*_a$) is small unless the surface area is very large ($S > \sim 10^2$ $\mu m^2/cm^3$). In the atmosphere, where significant nucleation has been observed, S is generally below 10^2 $\mu m^2/cm^3$. It should be noted that the nucleation rates observed in the atmosphere may depend strongly on the surface area of the preexisting particles because (1) preexisting particles have significant effect on

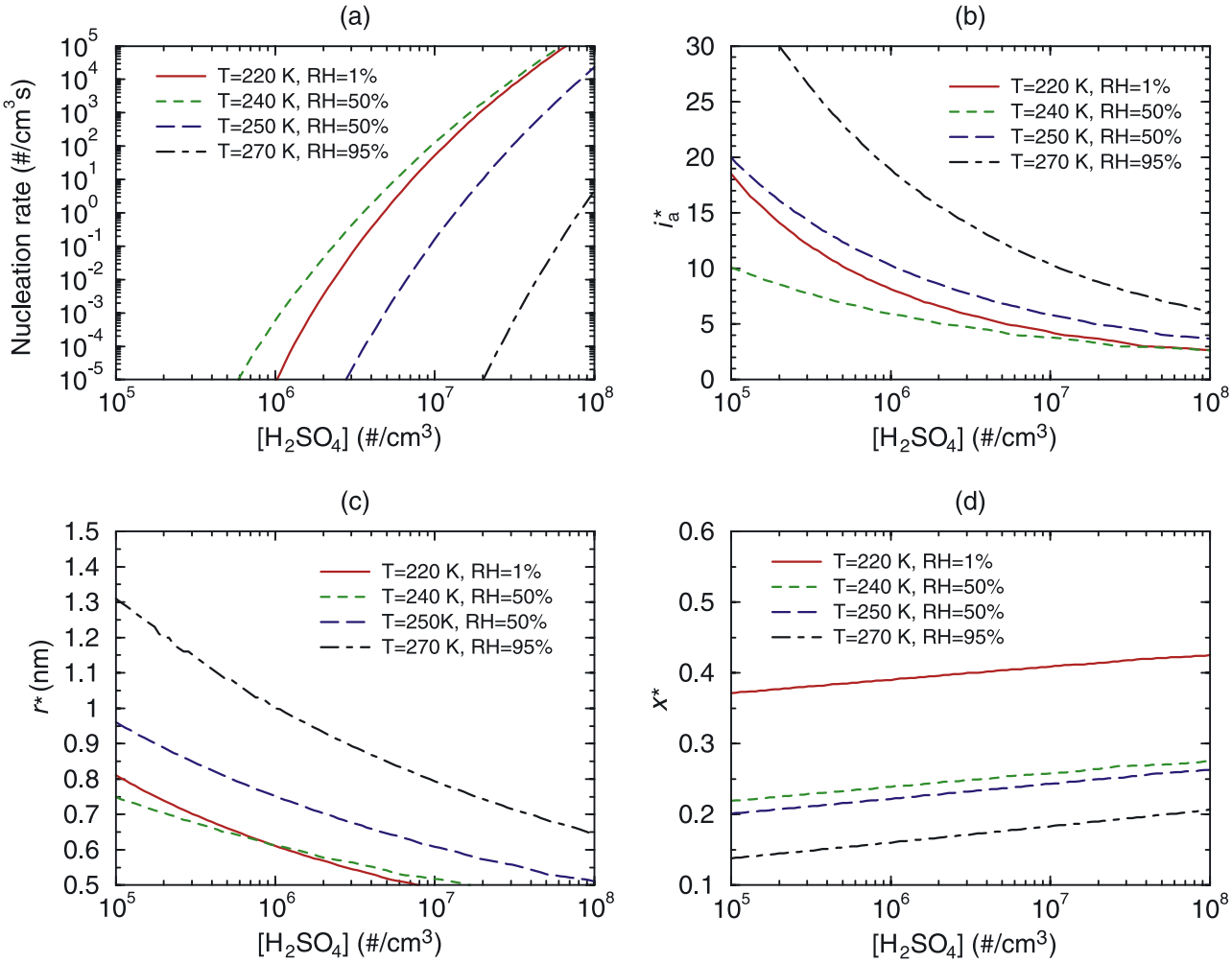

Figure 8. The dependence of (a) steady state nucleation rate, (b) number of H_2SO_4 molecules in the critical clusters (i_a^*), (c) critical radius (r^*), and (d) H_2SO_4 mole fraction (x^*) of the critical clusters on H_2SO_4 vapor concentration.

n_a to which the nucleation rate is very sensitive, (2) the observed particles are generally larger than 3 nm and the scavenging of clusters/particles smaller than 3 nm in size by preexisting particles may be important.

4. Look-Up Tables of Quasi-Unary H_2SO_4-H_2O Homogeneous Nucleation

[36] At a given condition, the classical binary nucleation theory predicts the nucleation rates from analytical formulas assuming a pseudo-steady state concentration of critical embryos. The kinetic QUN model calculates the nucleation rates (equation (13)) based on the cluster distributions simulated explicitly (equations (8)–(9)). In order to reduce the computational costs of the nucleation rate calculations, which are very important for multidimensional modeling and facilitate the quick estimation of the nucleation rates at given n_a, RH, and T, we generated the look-up tables for quasi-unary homogeneous nucleation rates (J'_{QUN}, at pseudo-steady state) and the properties of critical clusters (i_a^*, r^*, x^*). The effect of preexisting particles on nucleation rates is not considered here because at fixed n_a this effect is insignificant.

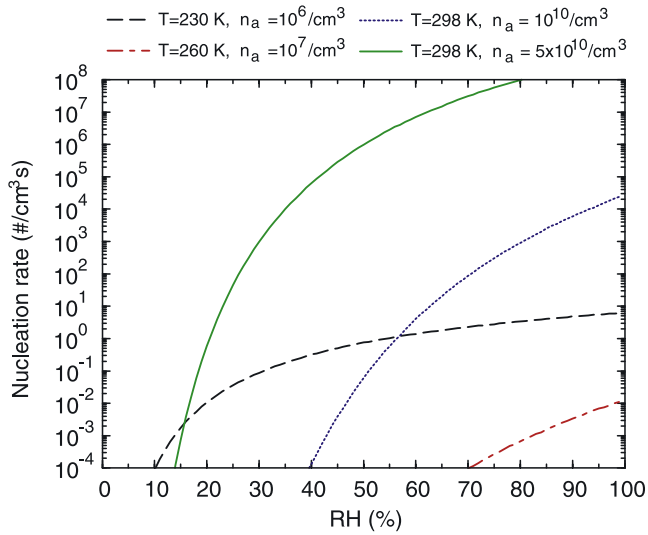

Figure 9. The dependence of kinetic quasi-unary nucleation rates on RH (at given T and n_a, S = 0 $\mu m^2/cm^3$).

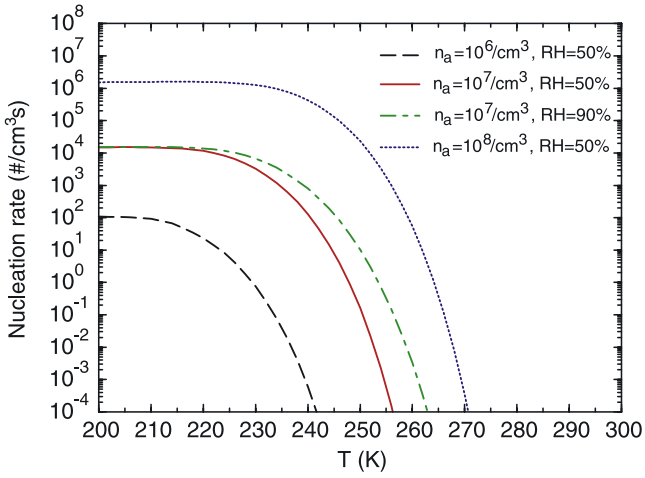

Figure 10. The dependence of kinetic quasi-unary nucleation rates on T (at given RH and n_a, $S = 0$ $\mu m^2/cm^3$).

[37] J'_{QUN}, i^*_a, r^*, and x^* depend on n_a, RH and T, and thus, the look-up tables are three-dimensional. In the background stratosphere and troposphere, n_a typically does not exceed $10^8/cm^3$ and ambient temperature can be as low as 180 K. In the laboratory conditions and some plumes from engine exhaust or power plants emissions, n_a can be in the range of 10^8–$10^{12}/cm^3$ and typical temperatures corresponding to these situations are above 280 K. Two separate look-up tables corresponding to these two different situations have been designed so that the tables have a good resolution in each dimension and their sizes are reasonable. Tables 1 and 2 show the range of each dimension, total number of points in each dimension, and values at each point for the look-up tables corresponding to conditions in the background atmosphere and laboratory studies/plumes, respectively.

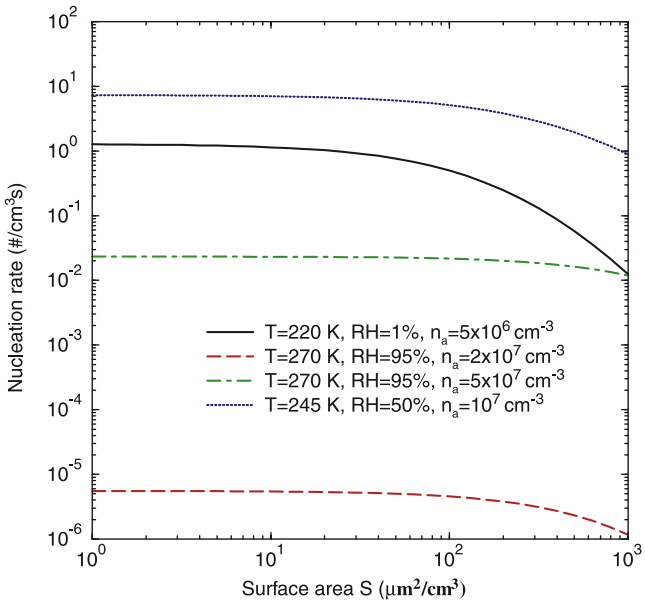

Figure 11. The dependence of kinetic quasi-unary nucleation rates on S (at given T, RH, and n_a).

Table 1. Range of Each Dimension, Total Number of Points in Each Dimension, and the Values at Each Point for the Look-Up Tables Corresponding to the Conditions in Background Atmosphere[a]

	Range	Total Number of Points	Values at Each Point
n_a, cm^{-3}	10^5–10^8	100	$n_a(i) = 10^5 \times 10^{(i-1)/33}$, $i = 1, 100$
T, K	180–300	61	$T(j) = 180 + 2 \times (j - 1)$, $j = 1, 61$
RH, %	1–99	99	$RH(k) = k$, $k = 1, 99$

[a]Here n_a is the total sulfuric acid molecule concentration (free + hydrated).

[38] At given values of $[H_2SO_4]$, T, and RH, the new particle formation rates of kinetic quasi-unary nucleation can be decided easily and efficiently using the look-up tables with a simple interpolation subroutine. The complete look up tables for J'_{QUN} ($[H_2SO_4]$, RH, T), i^*_a ($[H_2SO_4]$, RH, T), r^* ($[H_2SO_4]$, RH, T), and x^* ($[H_2SO_4]$, RH, T), along with a FORTRAN code to read and interpolate the tables, can be found in the auxiliary material.[1] Below we present subsets of look-up tables to illustrate the conditions, when H_2SO_4-H_2O homogeneous nucleation may become significant.

[39] Tables 3–5 are subsets of J'_{QUN}, i^*_a, r^* look-up tables at selected values of n_a, RH, and T under ambient atmosphere conditions. Nucleation rates are negligible, when i^*_a are very large. In the table, the values of i^*_a are set to 98 when $i^*_a > 98$ and the corresponding nucleation rates are set to minimum value ($10^{-30}/cm^3s$). The values of J'_{QUN} at selected temperatures are also plotted as contours in the RH versus n_a planes in Figure 12.

[40] Quasi-unary nucleation rates for H_2SO_4-H_2O system are larger at lower temperature, higher RH, or higher n_a. H_2SO_4-H_2O homogeneous nucleation is negligible in the boundary layer; however, it may be significant in the middle and upper troposphere. At very lower temperatures, J'_{QUN} may become independent of RH because the nucleation in such conditions (i.e., number of H_2SO_4 molecules in the critical clusters is less than 2) is barrierless and thus the nucleation rates are limited by the kinetic collision rates of H_2SO_4 monomers only. It should be noted that while J'_{QUN} can be very large at lower temperature even if n_a is small, the critical clusters are very small and it may take a long time for these clusters to grow to observable size (~3 nm) unless other species contribute to the growth of the nucleated clusters.

[41] Tables 6–8 are subsets of J'_{QUN}, i^*_a, r^* look-up tables for the conditions typical for the laboratory measurements and plumes. The corresponding J'_{QUN} contours in the RH versus n_a planes are shown in Figure 13. In order to observe significant H_2SO_4-H_2O homogeneous nucleation in the laboratory at room temperature (~300 K), n_a has to be above $10^{11}/cm^3$, when RH is small (<20%), and in the range of 10^{10}–$10^{11}/cm^3$ when RH is large. In the exhaust from motor vehicles burning fuel with sulfur content of 400 ppm, n_a in the exhaust just exiting the tailpipe can be

[1]Auxiliary material is available at ftp://ftp.agu.org/apend/jd/2005JD006358.

Table 2. Range of Each Dimension, Total Number of Points in Each Dimension, and the Values at Each Point for the Look-Up Tables Corresponding to the Conditions in Laboratory Studies/Plumes

	Range	Total Number of Points	Values at Each Point
n_a, cm^{-3}	10^8–10^{12}	133	$n_a(i) = 10^8 \times 10^{(i-1)/33}$, i = 1, 133
T, K	280–310	16	$T(j) = 280 + 2 \times (j - 1)$, j = 1, 16
RH, %	1–99	99	$RH(k) = k$, k = 1, 99

above 10^{12}/cm^3 and our study indicates that significant homogenous nucleation can happen in these vehicular exhausts (Du and Yu, submitted manuscript, 2006). It can also seen from Tables 7–8 that in the cases, when the nucleation rate is significant, the size of critical clusters ($i_a^* <\sim 15$, $r^* < 0.8$ nm) is small.

5. Summary and Discussion

[42] Gaseous H_2SO_4 and H_2O have very low vapor pressure over the binary H_2SO_4-H_2O solution and many observations indicate that most of the nucleation events observed in the atmosphere involve these two precursors. In the past half century, the classical binary H_2SO_4-H_2O homogeneous nucleation theory has been continuously developing and improving. However, the agreement between theories and experimental data is still often unsatisfactory. Recently, *Yu* [2005] showed that the binary homogeneous nucleation of H_2SO_4-H_2O can be treated as quasi-unary nucleation of H_2SO_4 in equilibrium with H_2O vapor and developed a kinetic H_2SO_4-H_2O nucleation model. The kinetic QUN model, which simulates cluster distributions kinetically and implicitly considers the hydration of clusters, is different from the classical BHN model, which assumes statistical equilibrium cluster distributions and accounts for the hydration of sulfuric acid monomers only.

[43] In this paper the QUN model has been improved through the incorporation of more robust thermodynamics of the cluster formation. The major revisions in the QUN model include the following: (1) Application of the Kelvin equation without the surface derivative term for the derivation of the cluster composition (water content); (2) Usage of H_2SO_4 partial molecular volume in the equation calculating evaporation rate; (3) Incorporation of the monomer hydration effect in calculating evaporation rates; (4) Monomer hydration is calculated with Kelvin equation that leads to better overall agreement of the predicted nucleation rates with experimental data; (5) Extension of the QUN model through the incorporation of the effect of the preexisting particles on the nucleation rates.

[44] We applied the revised QUN model to investigate the dependence of kinetically based H_2SO_4-H_2O homogeneous nucleation rates on key input parameters and determined conditions, in which the binary H_2SO_4-H_2O nucleation may be significant. On the basis of the detailed kinetic simulation carried out using the revised QUN model, we generated the look-up tables for nucleation rates and critical cluster properties, which cover a wide range of the key parameters typical for the background atmosphere, laboratory conditions and exhaust plumes. The look-up tables can be easily included in multidimensional models to predict BHN rates at very low computational costs and they can be used for the analysis and interpretation of the observed nucleation events.

[45] There exist uncertainties in the H_2SO_4-H_2O homogeneous nucleation rates calculated with the kinetic QUN

Table 3. Subsets of Nucleation Rate, cm^{-3} s^{-1} Look-Up Tables at Selected Values of n_a, C, in cm^{-3}, *RH,* %, and *T,* K, Under Background Atmosphere Conditions

RH\C	1.0E+05	1.0E+06	2.0E+06	4.0E+06	7.1E+06	1.0E+07	2.0E+07	4.0E+07	7.1E+07	1.0E+08
					T = 220 K					
1	2.7E-30	7.6E-06	3.5E-03	3.8E-01	9.1E+00	5.3E+01	1.2E+03	1.8E+04	1.2E+05	3.6E+05
20	3.6E-06	4.3E+00	5.4E+01	5.2E+02	2.6E+03	6.8E+03	4.0E+04	2.0E+05	6.8E+05	1.4E+06
40	2.5E-04	1.7E+01	1.5E+02	1.1E+03	4.5E+03	1.1E+04	5.2E+04	2.3E+05	7.5E+05	1.5E+06
60	1.9E-03	3.0E+01	2.3E+02	1.5E+03	5.6E+03	1.2E+04	5.7E+04	2.5E+05	7.8E+05	1.6E+06
80	4.6E-03	4.1E+01	3.0E+02	1.7E+03	6.2E+03	1.3E+04	6.0E+04	2.6E+05	8.0E+05	1.6E+06
					T = 240 K					
10	1.0E-30	1.7E-14	1.5E-09	4.3E-06	8.1E-04	1.4E-02	2.1E+00	1.3E+02	2.4E+03	1.2E+04
30	3.7E-24	3.3E-06	9.1E-04	9.5E-02	2.4E+00	1.5E+01	4.0E+02	7.1E+03	5.6E+04	1.8E+05
50	5.1E-16	5.9E-04	4.5E-02	1.9E+00	2.7E+01	1.3E+02	2.0E+03	2.5E+04	1.5E+05	4.3E+05
70	2.9E-12	8.3E-03	3.5E-01	9.5E+00	1.0E+02	3.9E+02	4.8E+03	4.7E+04	2.5E+05	6.5E+05
90	5.5E-10	4.3E-02	1.3E+00	2.6E+01	2.2E+02	8.0E+02	8.4E+03	7.0E+04	3.3E+05	8.3E+05
					T = 260 K					
10	1.0E-30	1.0E-30	1.0E-30	1.0E-30	1.0E-30	1.0E-30	1.7E-24	5.0E-16	5.7E-11	2.3E-08
30	1.0E-30	1.0E-30	2.0E-30	6.1E-21	1.3E-15	7.2E-13	2.5E-08	9.9E-05	2.3E-02	4.6E-01
50	1.0E-30	1.2E-25	8.9E-18	1.7E-12	3.6E-09	2.3E-07	2.8E-04	1.0E-01	5.6E+00	5.5E+01
70	1.0E-30	1.3E-17	1.8E-12	1.2E-08	3.9E-06	9.5E-05	2.7E-02	3.3E+00	9.3E+01	6.5E+02
90	1.0E-30	2.0E-13	1.6E-09	1.8E-06	2.3E-04	3.4E-03	4.2E-01	2.7E+01	5.3E+02	2.8E+03
					T = 280 K					
10	1.0E-30	1.0E-30	1.0E-30	1.0E-30	1.0E-30	1.0E-30	1.0E-30	1.0E-30	1.0E-30	1.0E-30
30	1.0E-30	1.0E-30	1.0E-30	1.0E-30	1.0E-30	1.0E-30	1.0E-30	1.0E-30	1.0E-30	5.1E-29
50	1.0E-30	1.0E-30	1.0E-30	1.0E-30	1.0E-30	1.0E-30	1.0E-30	3.0E-25	2.0E-18	5.9E-15
70	1.0E-30	1.0E-30	1.0E-30	1.0E-30	1.0E-30	1.0E-30	2.1E-23	5.1E-16	1.6E-11	3.7E-09
90	1.0E-30	1.0E-30	1.0E-30	1.0E-30	2.7E-28	1.5E-23	2.5E-16	4.7E-11	1.1E-07	7.1E-06
99	1.0E-30	1.0E-30	1.0E-30	1.0E-30	1.4E-24	1.7E-20	3.3E-14	1.7E-09	1.7E-06	7.8E-05

Table 4. Subsets of Look-Up Tables for the Number of H_2SO_4 Molecules in the Critical Clusters at Selected Values of n_a, C, in cm^{-3}, *RH,* %, and *T,* K, Under Background Atmosphere Conditions

RH\C	1.0E+05	1.0E+06	2.0E+06	4.0E+06	7.1E+06	1.0E+07	2.0E+07	4.0E+07	7.1E+07	1.0E+08
					T = 220 K					
1	1.8E+01	8.1E+00	6.6E+00	5.4E+00	4.7E+00	4.3E+00	3.7E+00	3.0E+00	2.8E+00	2.7E+00
20	5.0E+00	3.3E+00	2.9E+00	2.7E+00	2.4E+00	2.2E+00	2.0E+00	2.0E+00	2.0E+00	2.0E+00
40	4.0E+00	2.9E+00	2.6E+00	2.2E+00	2.0E+00	2.0E+00	2.0E+00	2.0E+00	2.0E+00	2.0E+00
60	3.7E+00	2.7E+00	2.3E+00	2.0E+00	2.0E+00	2.0E+00	2.0E+00	2.0E+00	2.0E+00	2.0E+00
80	3.4E+00	2.5E+00	2.0E+00	2.0E+00	2.0E+00	2.0E+00	2.0E+00	2.0E+00	2.0E+00	2.0E+00
					T = 240 K					
10	3.7E+01	1.5E+01	1.2E+01	9.3E+00	7.8E+00	7.1E+00	5.9E+00	4.9E+00	4.3E+00	3.9E+00
30	1.5E+01	7.7E+00	6.5E+00	5.5E+00	4.9E+00	4.5E+00	3.9E+00	3.4E+00	3.0E+00	2.9E+00
50	1.0E+01	5.9E+00	5.1E+00	4.5E+00	3.9E+00	3.8E+00	3.3E+00	2.9E+00	2.8E+00	2.6E+00
70	8.1E+00	5.0E+00	4.5E+00	3.9E+00	3.6E+00	3.4E+00	3.0E+00	2.8E+00	2.6E+00	2.3E+00
90	6.9E+00	4.6E+00	4.0E+00	3.7E+00	3.2E+00	3.0E+00	2.9E+00	2.6E+00	2.3E+00	2.0E+00
					T = 260 K					
10	9.8E+01	9.8E+01	9.8E+01	7.3E+01	5.2E+01	4.3E+01	3.0E+01	2.2E+01	1.7E+01	1.5E+01
30	9.8E+01	3.7E+01	2.8E+01	2.1E+01	1.7E+01	1.5E+01	1.2E+01	9.7E+00	8.2E+00	7.5E+00
50	4.8E+01	2.0E+01	1.6E+01	1.3E+01	1.1E+01	1.0E+01	8.4E+00	7.0E+00	6.1E+00	5.7E+00
70	2.9E+01	1.4E+01	1.2E+01	9.9E+00	8.7E+00	7.9E+00	6.8E+00	5.8E+00	5.0E+00	4.8E+00
90	2.1E+01	1.1E+01	9.6E+00	8.2E+00	7.2E+00	6.7E+00	5.8E+00	5.0E+00	4.5E+00	4.2E+00
					T = 280 K					
10	9.8E+01	9.8E+01	9.8E+01	9.8E+01	9.8E+01	9.8E+01	9.8E+01	9.8E+01	9.8E+01	9.8E+01
30	9.8E+01	9.8E+01	9.8E+01	9.8E+01	9.8E+01	9.8E+01	8.4E+01	5.6E+01	4.1E+01	3.5E+01
50	9.8E+01	9.8E+01	9.8E+01	7.5E+01	5.7E+01	4.8E+01	3.5E+01	2.6E+01	2.1E+01	1.9E+01
70	9.8E+01	7.1E+01	5.2E+01	3.9E+01	3.2E+01	2.8E+01	2.2E+01	1.7E+01	1.5E+01	1.3E+01
90	9.8E+01	4.1E+01	3.2E+01	2.6E+01	2.2E+01	1.9E+01	1.6E+01	1.3E+01	1.1E+01	1.0E+01
99	7.3E+01	3.4E+01	2.7E+01	2.2E+01	1.9E+01	1.7E+01	1.4E+01	1.2E+01	1.0E+01	9.3E+00

model, mainly due to the uncertainties in the calculated evaporation rates associated with the uncertainties in the cluster compositions, monomer hydration, and acid/water activities in the solution. To reduce the uncertainties, more accurate data on the thermodynamics of the monomer hydration and activities of H_2SO_4 and H_2O in the solution are needed. There also exist large uncertainties in the laboratory studies of H_2SO_4-H_2O homogeneous nucleation. Reduction of the uncertainties in the experimental data can help to identify the deficiency and improve the model of

Table 5. Subsets of Look-Up Tables for the Radius, cm, of the Critical Clusters at Selected Values of n_a, C, in cm^{-3}, *RH,* %, and *T,* K, Under Background Atmosphere Conditions

RH\C	1.0E+05	1.0E+06	2.0E+06	4.0E+06	7.1E+06	1.0E+07	2.0E+07	4.0E+07	7.1E+07	1.0E+08
					T = 220 K					
1	8.1E-08	6.1E-08	5.7E-08	5.3E-08	5.1E-08	4.9E-08	4.6E-08	4.3E-08	4.2E-08	4.1E-08
20	5.6E-08	4.7E-08	4.6E-08	4.4E-08	4.2E-08	4.1E-08	4.0E-08	4.0E-08	4.0E-08	4.0E-08
40	5.2E-08	4.6E-08	4.5E-08	4.2E-08	4.1E-08	4.1E-08	4.1E-08	4.1E-08	4.1E-08	4.1E-08
60	5.2E-08	4.6E-08	4.3E-08	4.1E-08	4.1E-08	4.1E-08	4.1E-08	4.1E-08	4.1E-08	4.1E-08
80	5.1E-08	4.5E-08	4.2E-08	4.2E-08	4.2E-08	4.2E-08	4.2E-08	4.2E-08	4.2E-08	4.2E-08
					T = 240 K					
10	1.1E-07	7.9E-08	7.3E-08	6.7E-08	6.3E-08	6.1E-08	5.7E-08	5.4E-08	5.1E-08	5.0E-08
30	8.3E-08	6.6E-08	6.2E-08	5.8E-08	5.6E-08	5.4E-08	5.1E-08	4.9E-08	4.6E-08	4.6E-08
50	7.5E-08	6.1E-08	5.8E-08	5.5E-08	5.3E-08	5.2E-08	4.9E-08	4.7E-08	4.6E-08	4.5E-08
70	7.1E-08	5.9E-08	5.6E-08	5.3E-08	5.2E-08	5.0E-08	4.8E-08	4.7E-08	4.5E-08	4.4E-08
90	6.8E-08	5.8E-08	5.5E-08	5.3E-08	5.0E-08	4.9E-08	4.8E-08	4.6E-08	4.4E-08	4.2E-08
					T = 260 K					
10	1.5E-07	1.5E-07	1.5E-07	1.4E-07	1.2E-07	1.1E-07	1.0E-07	9.0E-08	8.3E-08	7.9E-08
30	1.6E-07	1.2E-07	1.0E-07	9.4E-08	8.8E-08	8.4E-08	7.7E-08	7.1E-08	6.7E-08	6.5E-08
50	1.3E-07	9.7E-08	8.9E-08	8.2E-08	7.7E-08	7.5E-08	7.0E-08	6.5E-08	6.2E-08	6.0E-08
70	1.1E-07	8.7E-08	8.1E-08	7.6E-08	7.2E-08	7.0E-08	6.6E-08	6.2E-08	5.9E-08	5.7E-08
90	1.0E-07	8.2E-08	7.7E-08	7.2E-08	6.9E-08	6.7E-08	6.3E-08	5.9E-08	5.7E-08	5.5E-08
					T = 280 K					
10	1.5E-07	1.5E-07	1.5E-07	1.5E-07	1.5E-07	1.5E-07	1.5E-07	1.5E-07	1.5E-07	1.5E-07
30	1.6E-07	1.6E-07	1.6E-07	1.6E-07	1.6E-07	1.6E-07	1.5E-07	1.3E-07	1.2E-07	1.1E-07
50	1.7E-07	1.7E-07	1.7E-07	1.5E-07	1.4E-07	1.3E-07	1.2E-07	1.1E-07	9.7E-08	9.3E-08
70	1.8E-07	1.6E-07	1.4E-07	1.3E-07	1.2E-07	1.1E-07	1.0E-07	9.3E-08	8.7E-08	8.4E-08
90	1.9E-07	1.3E-07	1.2E-07	1.1E-07	1.0E-07	1.0E-07	9.3E-08	8.6E-08	8.1E-08	7.8E-08
99	1.7E-07	1.3E-07	1.2E-07	1.1E-07	1.0E-07	9.7E-08	9.0E-08	8.3E-08	7.9E-08	7.6E-08

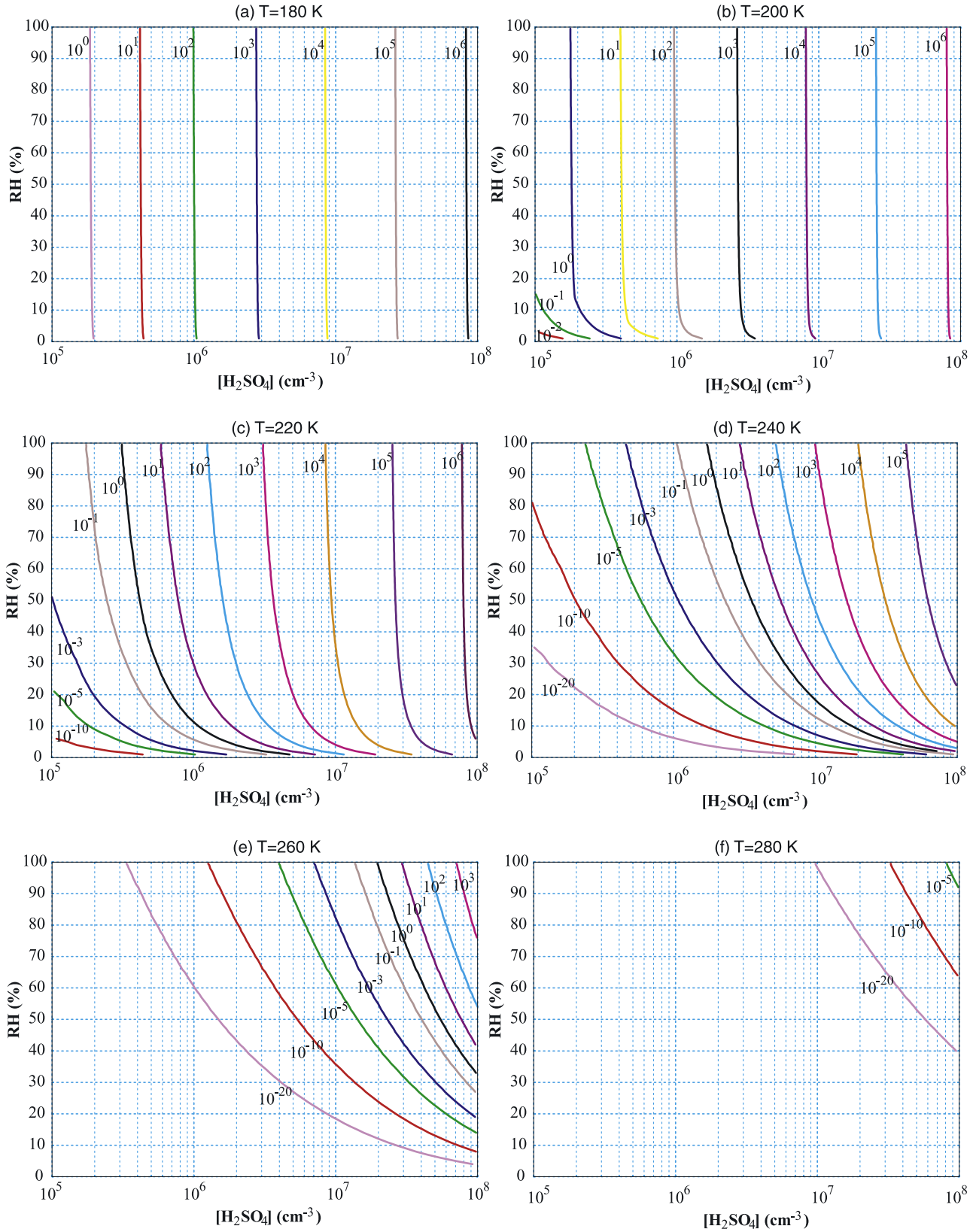

Figure 12. Contours of H_2SO_4-H_2O homogeneous nucleation rates based on kinetic quasi-unary nucleation model in the *RH* vs n_a planes under the conditions in laboratory studies/plumes: (a) $T = 180$ K, (b) $T = 200$ K, (c) $T = 220$ K, (d) $T = 240$ K, (e) $T = 260$ K, (f) $T = 280$ K. The numbers on the curves are the nucleation rates in $cm^{-3}s^{-1}$.

Table 6. Subsets of Nucleation Rate, $cm^{-3}s^{-1}$, Look-Up Tables at Selected Values of n_a, C, in cm^{-3}, *RH*, %, and *T*, K, Under Laboratory/Plume Conditions

RH\C	1.0E+08	5.0E+08	1.0E+09	5.0E+09	1.0E+10	5.0E+10	1.0E+11	5.0E+11	1.0E+12
					T = 280 K				
1	1.0E-30	1.0E-30	1.0E-30	1.0E-30	2.4E-30	1.7E-03	4.3E+02	7.2E+09	6.0E+11
10	1.0E-30	1.0E-30	9.2E-23	1.3E-04	4.0E+00	2.0E+07	1.8E+09	3.1E+12	3.6E+13
30	5.1E-29	6.4E-10	5.8E-05	2.6E+03	5.2E+05	4.2E+09	7.9E+10	1.6E+13	1.0E+14
50	5.9E-15	6.9E-04	1.2E+00	3.2E+05	1.8E+07	2.3E+10	2.7E+11	2.5E+13	1.3E+14
70	3.7E-09	4.2E-01	1.4E+02	3.6E+06	1.1E+08	5.5E+10	4.9E+11	3.2E+13	1.5E+14
90	7.1E-06	2.0E+01	2.6E+03	1.6E+07	3.3E+08	9.4E+10	7.1E+11	3.6E+13	1.7E+14
					T = 290 K				
1	1.0E-30	1.0E-30	1.0E-30	1.0E-30	1.0E-30	1.0E-30	2.2E-14	2.0E+04	1.4E+08
10	1.0E-30	1.0E-30	1.0E-30	2.2E-25	9.1E-14	3.3E+01	1.5E+05	4.5E+10	1.9E+12
30	1.0E-30	1.0E-30	1.0E-20	1.2E-04	2.2E+00	8.7E+06	8.3E+08	2.0E+12	2.5E+13
50	1.0E-30	8.5E-16	2.0E-09	8.6E+00	6.1E+03	3.5E+08	1.2E+10	6.6E+12	5.8E+13
70	6.9E-25	5.8E-09	1.4E-04	1.7E+03	2.9E+05	2.3E+09	4.9E+10	1.2E+13	8.6E+13
90	9.7E-17	2.7E-05	6.5E-02	3.7E+04	2.9E+06	7.5E+09	1.1E+11	1.8E+13	1.1E+14
					T = 300 K				
1	1.0E-30	1.0E-30	1.0E-30	1.0E-30	1.0E-30	1.0E-30	1.0E-30	1.8E-11	1.7E-01
10	1.0E-30	1.0E-30	1.0E-30	1.0E-30	1.0E-30	3.0E-13	8.2E-05	6.1E+06	3.8E+09
30	1.0E-30	1.0E-30	1.0E-30	1.5E-21	4.5E-12	3.5E+01	1.0E+05	2.6E+10	1.1E+12
50	1.0E-30	1.0E-30	2.6E-29	5.9E-09	1.1E-03	1.2E+05	3.2E+07	3.5E+11	7.2E+12
70	1.0E-30	1.1E-25	1.2E-16	1.1E-03	5.6E+00	6.9E+06	5.7E+08	1.4E+12	1.9E+13
90	1.0E-30	2.2E-16	3.1E-10	1.0E+00	7.9E+02	7.8E+07	3.5E+09	3.2E+12	3.4E+13

Table 7. Subsets of Look-Up Tables for the Number of H_2SO_4 Molecules in the Critical Clusters at Selected Values of n_a, C, in cm^{-3}, *RH,* %, and *T,* K, Under Laboratory/Plume Conditions

RH\C	1.0E+08	5.0E+08	1.0E+09	5.0E+09	1.0E+10	5.0E+10	1.0E+11	5.0E+11	1.0E+12
					T = 280 K				
1	9.8E+01	9.8E+01	9.8E+01	9.8E+01	6.4E+01	2.1E+01	1.4E+01	6.5E+00	4.9E+00
10	9.8E+01	5.7E+01	3.7E+01	1.6E+01	1.2E+01	6.5E+00	5.1E+00	3.2E+00	2.7E+00
30	3.5E+01	1.7E+01	1.3E+01	7.7E+00	6.2E+00	3.9E+00	3.4E+00	2.4E+00	2.0E+00
50	1.9E+01	1.1E+01	8.8E+00	5.7E+00	4.7E+00	3.2E+00	2.9E+00	2.0E+00	2.0E+00
70	1.3E+01	8.3E+00	6.9E+00	4.7E+00	4.0E+00	2.9E+00	2.6E+00	2.0E+00	2.0E+00
90	1.0E+01	6.8E+00	5.8E+00	4.0E+00	3.6E+00	2.7E+00	2.3E+00	2.0E+00	2.0E+00
					T = 300 K				
1	9.8E+01	9.8E+01	9.8E+01	9.8E+01	9.8E+01	9.8E+01	9.8E+01	4.1E+01	2.4E+01
10	9.8E+01	9.8E+01	9.8E+01	9.8E+01	9.8E+01	3.3E+01	2.2E+01	9.8E+00	7.3E+00
30	9.8E+01	9.8E+01	9.5E+01	3.5E+01	2.5E+01	1.2E+01	9.3E+00	5.4E+00	4.3E+00
50	9.8E+01	5.3E+01	3.7E+01	1.8E+01	1.4E+01	8.1E+00	6.5E+00	4.0E+00	3.5E+00
70	5.9E+01	2.9E+01	2.2E+01	1.3E+01	1.0E+01	6.3E+00	5.2E+00	3.5E+00	2.9E+00
90	3.4E+01	1.9E+01	1.6E+01	9.7E+00	8.0E+00	5.3E+00	4.5E+00	3.0E+00	2.8E+00

Table 8. Subsets of Look-Up Tables for the Radius, cm, of the Critical Clusters at Selected Values of n_a, C, in cm^{-3}, *RH,* %, and *T,* K, Under Laboratory/Plume Conditions

RH\C	1.0E+08	5.0E+08	1.0E+09	5.0E+09	1.0E+10	5.0E+10	1.0E+11	5.0E+11	1.0E+12
					T = 280 K				
1	1.4E-07	1.4E-07	1.4E-07	1.4E-07	1.2E-07	8.2E-08	7.2E-08	5.6E-08	5.0E-08
10	1.5E-07	1.2E-07	1.1E-07	8.0E-08	7.2E-08	5.8E-08	5.4E-08	4.5E-08	4.3E-08
30	1.1E-07	8.7E-08	7.9E-08	6.5E-08	6.0E-08	5.1E-08	4.8E-08	4.2E-08	4.0E-08
50	9.3E-08	7.6E-08	7.0E-08	6.0E-08	5.6E-08	4.8E-08	4.6E-08	4.1E-08	4.1E-08
70	8.4E-08	7.1E-08	6.6E-08	5.7E-08	5.3E-08	4.7E-08	4.5E-08	4.1E-08	4.1E-08
90	7.8E-08	6.7E-08	6.3E-08	5.4E-08	5.2E-08	4.7E-08	4.4E-08	4.2E-08	4.2E-08
					T = 300 K				
1	1.4E-07	1.4E-07	1.4E-07	1.4E-07	1.4E-07	1.4E-07	1.4E-07	1.0E-07	8.6E-08
10	1.5E-07	1.5E-07	1.5E-07	1.5E-07	1.5E-07	1.0E-07	8.8E-08	6.7E-08	6.0E-08
30	1.6E-07	1.6E-07	1.6E-07	1.1E-07	9.8E-08	7.6E-08	6.9E-08	5.6E-08	5.2E-08
50	1.7E-07	1.3E-07	1.2E-07	9.1E-08	8.3E-08	6.7E-08	6.2E-08	5.2E-08	4.9E-08
70	1.5E-07	1.1E-07	1.0E-07	8.2E-08	7.5E-08	6.3E-08	5.9E-08	5.1E-08	4.7E-08
90	1.2E-07	1.0E-07	9.2E-08	7.6E-08	7.1E-08	6.0E-08	5.7E-08	4.8E-08	4.7E-08

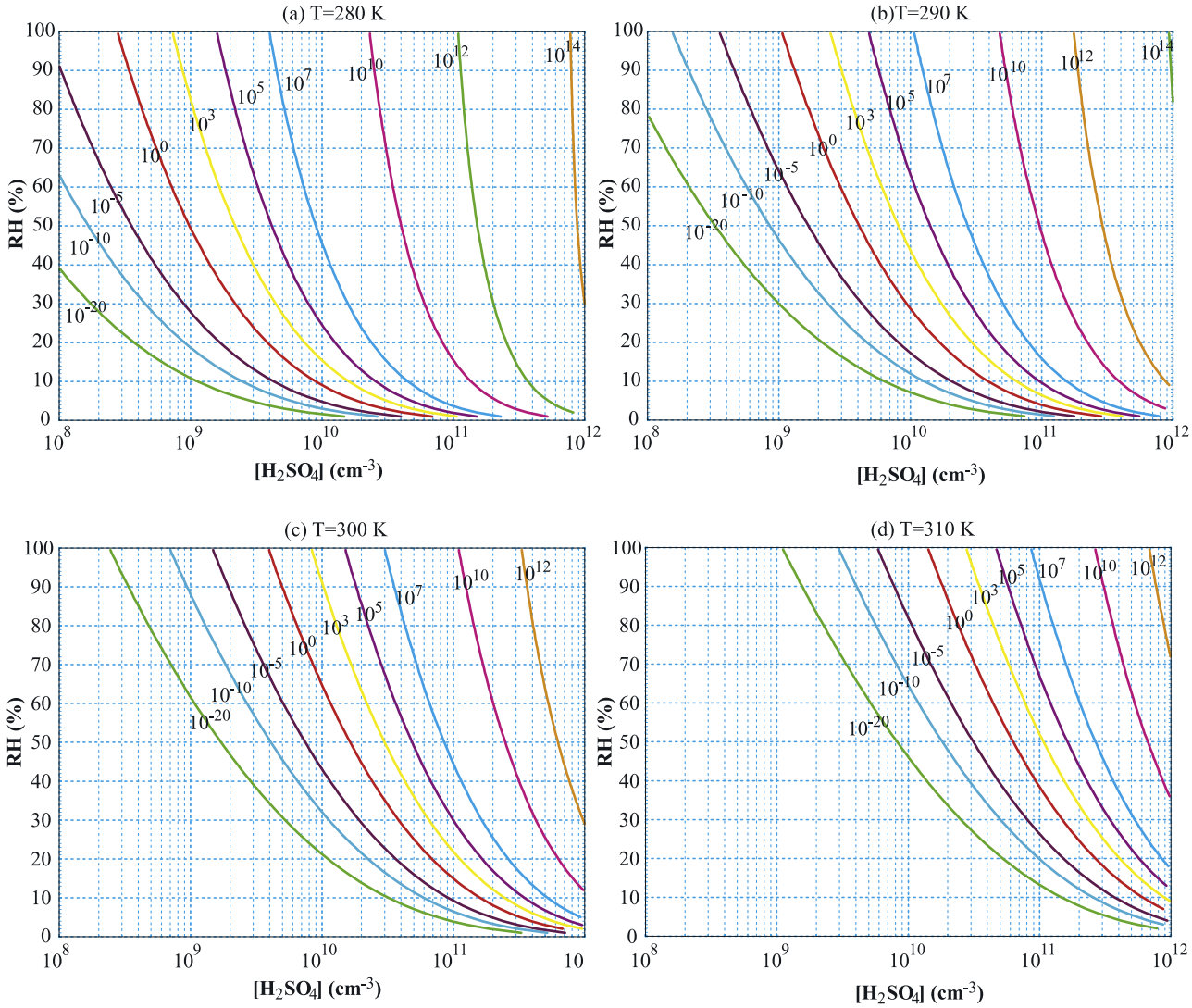

Figure 13. Contours of H_2SO_4-H_2O homogeneous nucleation rates based on kinetic quasi-unary nucleation model in the *RH* versus n_a planes under the conditions in laboratory studies/plumes: (a) T = 280 K, (b) T = 290 K, (c) T = 300 K, and (d) T = 310 K. The numbers on the curves are the nucleation rates in cm^{-3} s^{-1}.

H_2SO_4-H_2O homogeneous nucleation on which all recently proposed nucleation mechanisms, including ion-mediated nucleation, ternary nucleation, and organic enhanced nucleation, are based.

[46] **Acknowledgments.** This work was supported by the NSF under grant ATM 0104966 and New York State Energy Resource and Development Agency (NYSERDA). The author thanks one anonymous referee for very constructive comments.

References

Adams, P. J., and J. H. Seinfeld (2002), Predicting global aerosol size distributions in general circulation models, *J. Geophys. Res.*, *107*(D19), 4370, doi:10.1029/2001JD001010.

Andronache, C., et al. (1997), Gas-to-particle conversion of tropospheric sulfur as estimated from observations in the western North Pacific during PEM-West B, *J. Geophys. Res.*, *102*(D23), 28,511–28,538.

Ayers, G. P., R. W. Gillett, and J. L. Gras (1980), On the vapor pressure of sulfuric acid, *Geophys. Res. Lett.*, *7*, 433–436.

Ball, S. M., D. R. Hanson, F. L. Eisele, and P. H. McMurry (1999), Laboratory studies of particle nucleation: Initial results for H_2SO_4, H_2O, and NH_3 vapors, *J. Geophys. Res.*, *104*(D19), 23,709–23,718.

Boulaud, D., G. Madelaine, D. Vigla, and J. Bricard (1977), Experimental study on the nucleation of water vapor sulfuric acid binary system, *J. Chem. Phys.*, *66*, 4854–4860.

Capaldo, K. P., P. Kasibhatla, and S. N. Pandis (1999), Is aerosol production within the remote marine boundary layer sufficient to maintain observed concentrations?, *J. Geophys. Res.*, *104*(D3), 3483–3500.

Clarke, A. D., V. N. Kapustin, F. L. Eisele, R. J. Weber, and P. H. McMurry (1999), Particle production near marine clouds: Sulfuric acid and predictions from classical binary nucleation, *Geophys. Res. Lett.*, *26*(16), 2425–2428.

Clegg, S. L., and P. Brimblecombe (1995), Application of a multicomponent thermodynamic model to activities and thermal properties of 0–40 mol kg^{-1} aqueous sulfuric acid from <200 to 328 K, *J. Chem. Eng. Data*, *40*, 43–64.

Coffman, D. J., and D. A. Hegg (1995), A preliminary study of the effect of ammonia on particle nucleation in the marine boundary layer, *J. Geophys. Res.*, *100*, 7147–7160.

Doyle, G. J. (1961), Self-nucleation in the sulfuric acid-water system, *J. Chem. Phys.*, *35*, 795–799.

Eichkorn, S., S. Wilhelm, H. Aufmhoff, K. H. Wohlfrom, and F. Arnold (2002), Cosmic ray-induced aerosol-formation: First observational evidence from aircraft-based ion mass spectrometer measurements in the upper troposphere, *Geophys. Res. Lett.*, *29*(14), 1698, doi:10.1029/2002GL015044.

ENVIRON (2004), *Comprehensive Air Quality Model With Extensions (CAMx) Version 4.10s User's Guide*, ENVIRON Int. Corp., Novato, Calif.

Hamill, P., R. P. Turco, C. S. Kiang, O. B. Toon, and R. C. Whitten (1982), An analysis of various nucleation mechanisms for sulfate particles in the stratosphere, *J. Aerosol Sci.*, *13*, 561–585.

Heist, R. H., and H. Reiss (1974), Hydrates in supersaturated binary sulfuric acid-water vapor, *J. Chem. Phys.*, *61*, 573–581.

Jacobson, M. Z., R. P. Turco, E. Jensen, and O. Toon (1994), Modeling coagulation among particles of different composition and size, *Atmos. Environ.*, *28*, 1327–1338.

Jaecker-Voirol, A., P. Mirabel, and H. Reiss (1987), Hydrates in supersaturated binary sulfuric acid–water vapor: A reexamination, *J. Chem. Phys.*, *87*, 4849–4852.

Kazil, J., and E. R. Lovejoy (2004), Tropospheric ionization and aerosol production: A model study, *J. Geophys. Res.*, *109*, D19206, doi:10.1029/2004JD004852.

Korhonen, P. M., et al. (1999), Ternary nucleation of H_2SO_4, NH_3, and H_2O in the atmosphere, *J. Geophys. Res.*, *104*, 26,349–26,353.

Kreidenweis, S., and J. H. Seinfeld (1988), Nucleation of sulfuric acid-water and methanesulfonic acid- water solution particles: implications for the atmospheric chemistry of organosulfur species, *Atmos. Environ.*, *22*, 283–296.

Kulmala, M., and A. Laaksonen (1990), Binary nucleation of water–sulfuric acid system: Comparison of classical theories with different H_2SO_4 saturation vapor pressures, *J. Chem. Phys.*, *93*, 696–701.

Kulmala, M., A. Laaksonen, and S. L. Gershick (1992), The self-consistency correction to homogeneous nucleation: Extension to binary systems, *J. Aerosol Sci.*, *23*, 309–312.

Kulmala, M., A. Laaksonen, and L. Pirjola (1998), Parameterizations for sulfuric acid/water nucleation rates, *J. Geophys. Res.*, *103*, 8301–8308.

Laakso, L., J. M. Mäkelä, L. Pirjola, and M. Kulmala (2002), Model studies on ion-induced nucleation in the atmosphere, *J. Geophys. Res.*, *107*(D20), 4427, doi:10.1029/2002JD002140.

Laaksonen, A., R. McGraw, and H. Vehkamäki (1999), Liquid-drop formalism and free-energy surfaces in binary homogeneous nucleation theory, *J. Chem. Phys.*, *111*, 2019–2027.

Lee, S.-H., et al. (2003), New particle formation by ion-induced nucleation in the upper troposphere and lower stratosphere, *Science*, *26*, 1886–1889.

Mirabel, P., and J. L. Katz (1974), Binary homogeneous nucleation as a mechanism for the formation of aerosols, *J. Chem. Phys.*, *60*, 1138–1144.

Mirabel, P., and H. Reiss (1987), Resolution of the "Renninger-Wilemski Problem" concerning the identification of heteromolecular nuclei, *Langmuir*, *3*, 228–234.

Nadykto, A., and F. Yu (2005), Simple correction to the classical theory of homogeneous nucleation, *J. Chem. Phys.*, *122*, 104511.

Napari, I., M. Noppel, H. Vehkamäki, and M. Kulmala (2002), Parametrization of ternary nucleation rates for H_2SO_4-NH_3-H_2O vapors, *J. Geophys. Res.*, *107*(D19), 4381, doi:10.1029/2002JD002132.

Noppel, M., H. Vehkamaki, and M. Kulmala (2002), An improved model for hydrate formation in sulfuric acid–water nucleation, *J. Chem. Phys.*, *116*, 218–228.

Reiss, H. (1950), The kinetics of phase transition in binary systems, *J. Chem. Phys.*, *18*, 840–848.

Renninger, R. G., F. C. Hiller, and R. C. Bone (1981), Comment on "Self-nucleation in the sulfuric acid–water system," *J. Chem. Phys.*, *75*, 1584.

Russell, L. M., S. N. Pandis, and J. H. Seinfeld (1994), Aerosol production and growth in the marine boundary layer, *J. Geophys. Res.*, *99*, 20,989–21,003.

Taleb, D.-E., J.-L. Ponche, and P. Mirabel (1996), Vapor pressures in the ternary system water-nitric acid-sulfuric acid at low temperature: A re-examination, *J. Geophys. Res.*, *101*, 25,967–25,977.

Vehkamäki, H., et al. (2002), An improved parameterization for sulfuric acid–water nucleation rates for tropospheric and stratospheric conditions, *J. Geophys. Res.*, *107*(D22), 4622, doi:10.1029/2002JD002184.

Viisanen, Y., M. Kulmala, and A. Laaksonen (1997), Experiments on gas-liquid nucleation of sulfuric acid and water, *J. Chem. Phys.*, *107*, 920–926.

Wexler, A. S., F. W. Lurmann, and J. H. Seinfeld (1994), Modelling urban and regional aerosols—I. model development, *Atmos. Environ.*, *28*, 531–546.

Wilemski, G. (1975), Binary nucleation. I. Theory applied to water–ethanol vapors, *J. Chem. Phys.*, *62*, 3763–3771.

Wilemski, G. (1987), Revised classical binary nucleation theory for aqueous alcohol and acetane vapors, *J. Phys. Chem.*, *91*, 2492–2498.

Wilemski, G., and B. E. Wyslouzil (1995), Binary nucleation kinetics. I. Self-consistent size distribution, *J. Chem. Phys.*, *103*, 1127–1136.

Wilhelm, S., S. Eichkorn, D. Wiedner, L. Pirjola, and F. Arnold (2004), Ion-induced aerosol formation: new insights from laboratory measurements of mixed cluster ions HSO_4^- $(H_2SO_4)_a$ $(H_2O)_w$ and H^+ $(H_2SO_4)_a$ $(H_2O)_w$, *Atmos. Environ.*, *38*, 1735–1744.

Wyslouzil, B. E., J. H. Seinfeld, R. C. Flagan, and K. Okuyama (1991), Binary nucleation in acid–water systems. II. Sulfuric acid–water and a comparison with methanesulfonic acid–water, *J. Chem. Phys.*, *94*, 6842–6850.

Yu, F. (2002), Altitude variations of cosmic ray induced production of aerosols: Implications for global cloudiness and climate, *J. Geophys. Res.*, *107*(A7), 1118, doi:10.1029/2001JA000248.

Yu, F. (2005), Quasi-unary homogeneous nucleation of H_2SO_4-H_2O, *J. Chem. Phys.*, *122*, 074501.

Yu, F., and R. P. Turco (2000), Ultrafine aerosol formation via ion-mediated nucleation, *Geophys. Res. Lett.*, *27*, 883–886.

Yu, F., and R. P. Turco (2001), From molecular clusters to nanoparticles: The role of ambient ionization in tropospheric aerosol formation, *J. Geophys. Res.*, *106*, 4797–4814.

Zeleznik, F. J. (1991), Thermodynamic properties of the aqueous sulfuric acid system to 350 K, *J. Phys. Chem. Ref. Data*, *20*, 1157–1200.

Zhang, R., et al. (2004), Atmospheric new particle formation enhanced by organic acids, *Science*, *304*, 1487–1490.

F. Yu, Atmospheric Sciences Research Center, State University of New York at Albany, 251 Fuller Road, Albany, NY 12203, USA. (yfq@asrc.cestm.albany.edu)